THE EFFECTS OF CREEP ON THE STRUCTURE AND MECHANICAL PROPERTIES OF ZIRCONIUM

by

Charles Robert Mullen Jr.

A THESIS

submitted to

OREGON STATE COLLEGE

in partial fulfillment of
the requirements for the
degree of

MASTER OF SCIENCE

June 1960

APPROVED:

Redacted for privacy

Professor of Mechanical Engineering

In Charge of Major

Redacted for privacy

Head of Department

Redacted for privacy

Chairman of School Graduate Committee

Redacted for privacy

Dean of Graduate School

Date thesis is presented 10-6-53

Typed by Mrs. C. R. Mullen

ACKNOWLEDGEMENT

I would like to very sincerely thank Professor Olaf Paasche for his helpful suggestions and patience. My appreciation is also extended to Miss Ruth Marshall for her proof reading and helpful suggestions on grammatical structure.

I would also like to thank Mrs. C. R. Mullen and Miss Lucile Miles for typing, and finishing of the thesis.

Last, but not least, I am very grateful to the Oregon State College Engineering experiment station and Professor Phillip Osborne for making this research possible.

TABLE OF CONTENTS

LIST OF FIGURES

TABLES

INTRODUCTION

Much of the interest in zirconium today stems from its use in nuclear power reactors. Such an application of a metal requires certain properties and raises questions as to how the metal will withstand the conditions within a reactor.

The structural material of nuclear reactors may be in contact with heat transfer fluids, which implies that it must have good corrosion resistance, and because of the elevated temperature from the heat transfer fluids, the structure must also have good, moderate temperature mechanical properties. Also the structural material should have appropriate nuclear properties, i.e., some parts of the structure of the reactor must have a low neutron cross-section. Zirconium has all of the above properties besides being fairly easy to fabricate.

Zirconium, in use in reactors, is under stress and at the same time may be at elevated temperatures for varying periods of time, due to heat transfer fluids. Under these conditions zirconium will be subject to creep, which is defined as the elongation of a structure under constant stress for fairly long periods of time and is usually perceived only at elevated temperatures, where the process is markedly increased.

Thus, during the lifetime of a reactor it will be important to know what effects, if any, the creep

phenomena has had on the structural material of the reactor. If there are any changes, what properties have changed, and how will they affect the operation of the reactor? In order to design metals and alloys for future use in reactors, it will be essential to know what changes in metallic structure have brought about the changes in mechanical properties and to know by what mechanism the metallic structure was changed.

This research was concerned with the above problems; its object was to determine the effects of prior creep on the mechanical properties and structure of reactor grade zirconium.

THE EFFECTS OF CREEP ON THE STRUCTURE AND MECHANICAL PROPERTIES OF ZIRCONIUM

CREEP THEORY

Creep may be defined as the time-dependant part of the deformation which accompanies the application of stress to a solid.

The action of creep is divided into three distinct parts, characterized by a creep curve, which is a strain versus time curve.

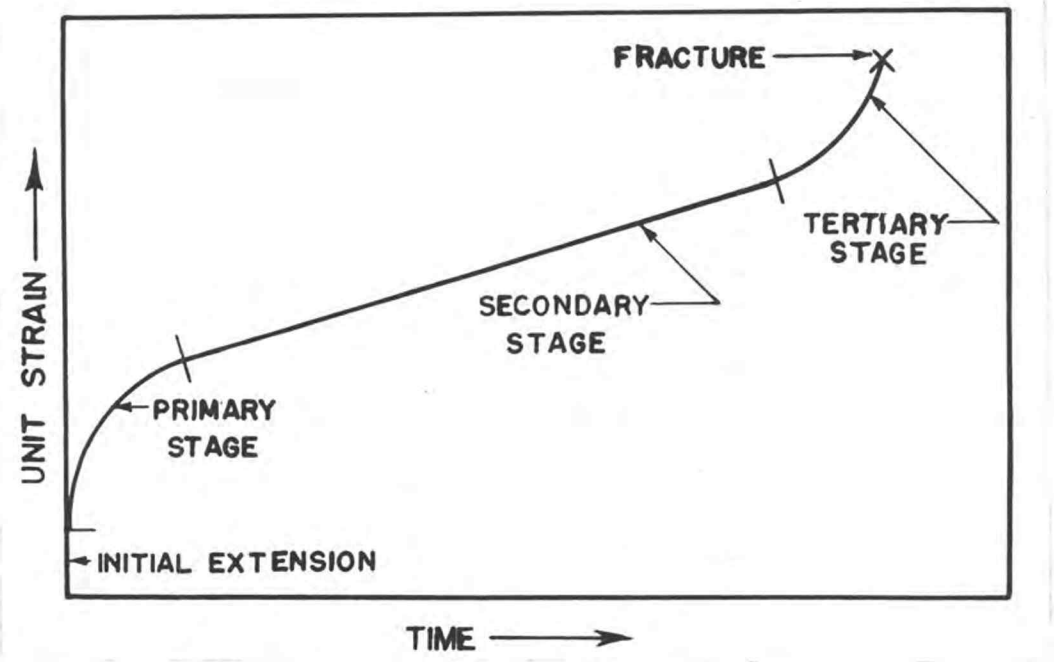

Figure 1 Typical Creep Curve

Figure 1 shows a typical creep curve. When the load is first applied there is an instantaneous elongation, which is followed by the first stage of creep, called transient creep and characterized by a gradually decreasing

rate of strain. Second stage creep shows a constant rate of strain; the term minimum creep rate refers to the second stage creep rate. This second stage is usually called quasi-viscous creep and will be discussed later. The third stage, or tertiary creep, has an accelerated strain rate which leads to fracture.

The first and third stages are usually accompanied by slip bands which would indicate that the mechanism of deformation is the same as would be found in tensile testing at ordinary temperature. It is commonly agreed that the transient creep mechanism is not very different from that of an ordinary tensile test. Some investigators think that the third stage, which is accelerating, is not truly a creep phenomena because of the change in stress due to a large change in cross-sectional area.

Quasi-viscous creep, however, seems to take place by either viscous flow or by slipless flow, according to the temperature and loading of the metal. The result of viscous flow is grain boundary creep. It results in no deformation of the grains, but the grains seem to shift to a limited extent until they interlock or draw together. Slipless flow, on the other hand, is characterized by a complete absence of slip bands, suggesting that slip has not occurred; however, Hansen and Wheeler (14) have found that the large deformation in the quasi-

viscous portion of the creep curve cannot be accounted for entirely by grain boundary movement, and some strain hardening has been observed. Only slip is known to produce strain hardening; so it appears that slipless flow may actually involve slip. This means that slip is less extensive or that it takes place on many different planes individually rather than in clusters and is, therefore, unobservable. It has also been found that coarse grain size favors normal slip and fine grain size favors slipless flow. This suggests that grain boundaries strongly influence the creep mechanism.

It would be advantageous now to investigate the observable mechanisms of deformation and their modification due to creep conditions.

Metals under ordinary temperature and stress have essentially two observable mechanisms for deformation; slip and twinning. Under the conditions of creep, these mechanisms are modified. It has been found by Hansen and Wheeler (14) in their work with aluminum that the metallographic changes accompanying creep in a polycrystalline material depend upon whether the temperature at which the tests were carried out was high or low.

In general, at high temperature the formation of slip bands is almost unobservable, except in crystals near the edges of the specimen. A change, however,

occurs in the grain boundary during transient creep; the boundary becomes more pronounced, especially on boundaries at right angles to the direction of applied stress. During the early quasi-viscous portion of creep no more grain boundary movement is noticed, but later further changes occur at the boundaries and signs of movement around the boundaries occur. No signs of slip occur during this portion of creep, whereas slip is marked in a specimen under the same condition but loaded rapidly.

At low temperature the deformation of polycrystalline aggregates proceeds in quite a different manner from those for the high temperature. This deformation is very similar to deformation observed under a faster loading at ordinary conditions. Slip bands are observed and some movement of the grain boundaries is observed but nothing like that for the high temperature creep.

The work of Jenkins and Meller (16) tends to support the above phenomena, i.e., at high temperature creep was accompanied by modification of the structure at the crystal boundaries, leading to the formation of intercrystalline fissures and intercrystalline fracture, while at low temperature, the mechanism of deformation was by slip and transcrystalline failure.

Now, one may ask the question, how does slip or

twinning take place, or what is its mechanism? In order to answer this question by the most recent theories, the concept of dislocations must be introduced.

The above discussion was related to and explained the observable effects of deformation of a metal. It is, however, far from adequate in accounting for the stresses that are required to make metals flow. If slip is thought of as a homogeneous shearing of planes of atoms within a crystal in which all the atoms in adjacent planes move simultaneously, the stresses necessary to cause slip can be estimated by multiplying the shear by the shear modulus. A value of from 1,000 to 10,000 times the observed value of shearing yield strength is obtained. This, as well as other things, has led to many new important theories concerned with the plastic properties of materials. The dislocation theory is one of these.

A dislocation is simply a defect in the periodicity of the atomic lattice and viewed three-dimensionally may be visualized as one more vertical plane of atoms existing above a horizontal plane (the slip plane) than there is below the slip plane. This type of dislocation is known as an edge dislocation and is the simplest type. This extra plane of atoms tends to set up a stress field in the area of the dislocation. Under the influence of an applied shear stress the dislocation may move by the process of only a single line of atoms (the dislocation

line moving at any instant. The direction of propogation (direction of movement) and the applied shear stress are collinear and both perpendicular to the dislocation line of an edge dislocation.

Other types of dislocations have also been found. One of these is the screw dislocation which was first proposed by Burgers. Its line of dislocations and slip direction are collinear and perpendicular to the direction of propogation. The details of this and other types of dislocations can be found in other literature (2).

It is thought that dislocations originate at points of imperfection and exist in large numbers even in the most carefully annealed crystals. Accidents of crystal growth result in domains within crystals with slightly different orientation which constitute possible sources of dislocations. Taylor postulated that there were positive and negative dislocations and ones with opposite signs tend to attract each other and ones with like signs repell each other. When two dislocations of opposite signs came together, they tended to cancel each other.

The potential energy of a dislocation is actually a measure of its ability to move within the crystal, i.e. its energy in a stable crystal must be increased before it will move. This energy is known as the activation

energy.

There is a probability that thermal fluctuation may be great enough that the dislocation could move without application of an external load. Also, this probability increases exponentially with temperature. At high temperatures there is great probability that the diffusion of dislocations due to thermal activation energy enables dislocations to surmount potential barriers.

If the material is stressed this, too, will tend to lower the potential barrier and make diffusion or movement of the dislocation possible.

Slip, therefore, is caused by the movement of the dislocations, and is dependent on both stress and temperature.

The above theory was developed by Taylor, Orowan and Polanyi as outlined by Sulley (2) and when first developed had remarkable success. It had certain short comings, however, one of which was the explanation of the presence of slip bands. The shear due to the movement of dislocation is of the order of an interatomic spacing and, therefore, would not be visible. Some other mechanism must be sought to explain the much larger slip bands.

The Frank-Read spiral mechanism or source has been proposed to explain how dislocations might multiply and

this would increase the effectiveness as much as a thousandfold. This mechanism is too complicated to explain here but may be found in many metallurgical text books and journals.

It has also been shown that it is unlikely that viscous flow in the grain boundaries can make any major contribution to creep, since only small movements in grain boundaries are permitted before the grains interlock and make movement more difficult. The greater difficulty of detecting slip bands in creep tests made at elevated temperature suggests that slip occurs by smaller movement and with a larger number of slip bands.

Wood, Tapsell (27) and Crussard (7) have shown by x-ray evidence that at high temperature where grain boundary phenomena occurs, creep is accompanied by little distortion of the lattice through the breakdown of the crystals to smaller units. At low temperature, where the boundaries are rigid, the change in x-ray spectra brought about by creep are similar to those caused by fast deformation, indictive of much distortion of the lattice accompanying slip and crystallite formation.

In summing up the theory of creep in simplest form, we have certain visible phenomena such as slip bands and twinning and from this, theories have been postulated, most of them containing the idea of dislocation.

1. When deformation rate is relatively high, such as in tensile tests, deformation takes place by normal slip. Twinning may also occur but it is a minor factor as compared to normal slip.
2. When the deformation rate is fairly low, such as would be encountered in most industrial applications, the mechanism of creep is slipless flow. Slipless flow is favored by relatively high temperature, light loads, and fine grain size. The larger the grains the more the tendency is to form slip bands. Slipless flow may be called the interaction between viscous flow and slip. Viscous flow is a result of grain boundary creep and only occurs in grain boundary regions.
3. When the deformation is very low, the deformation mechanism is almost entirely viscous flow or grain boundary flow. It is a much smaller deformation than slip, but will take place sometimes when the stress is not high enough to cause slip.
4. The transient creep mechanism is not much different from that of an ordinary tensile

test.

5. The quasi-viscous stage of creep is similar to the transient stage but at a lower strain rate and slip occurs by smaller movement and with a large number of individual slip bands which makes them unobservable.
6. Tertiary creep, or third stage creep, is thought by many not to be a true creep phenomena, but very little is known about this stage.

Specimens

The material used for specimens was acquired from the U. S. Bureau of Mines, Albany, Oregon. The zirconium used was arc melted sponge zirconium cold swaged to 3/8 inch diameter rods. Three lots of specimens were used. The parts per million of impurities are listed below for all three lots:

Element	Parts per Million		
	#1	#2	#3
Aluminum	55	55	300
Boron	0.7	0.9	0.5
Cadmium	0.5	0.5	0.5
Chromium	20	40	120
Cobalt	20	20	5
Copper	25	20	60
Iron	470	435	460
Lead	40	35	30
Magnesium	15	15	8
Manganese	10	10	13
Molybdenum	20	20	10
Nickel	5	5	10
Nitrogen	0.015	...	...
Silicon	45	50	200
Tin	55	90	500
Titanium	20	25	...
Vanadium	20	20	20

Fig. 2 is a drawing with dimensions of the specimen. No testing was done with the first rod due to machining difficulties. Nineteen specimens were machined from the second rod and eleven from the third. Each specimen had a 2 inch gage length with approximately 3/8 inch on each side of the gage length for clearance in

tensile testing; the diameters were machined to 0.252 inch ± 0.002. The second rod adhered to this very closely, but the third rod had a larger deviation than ± 0.002 which can be seen from the data, Table I.

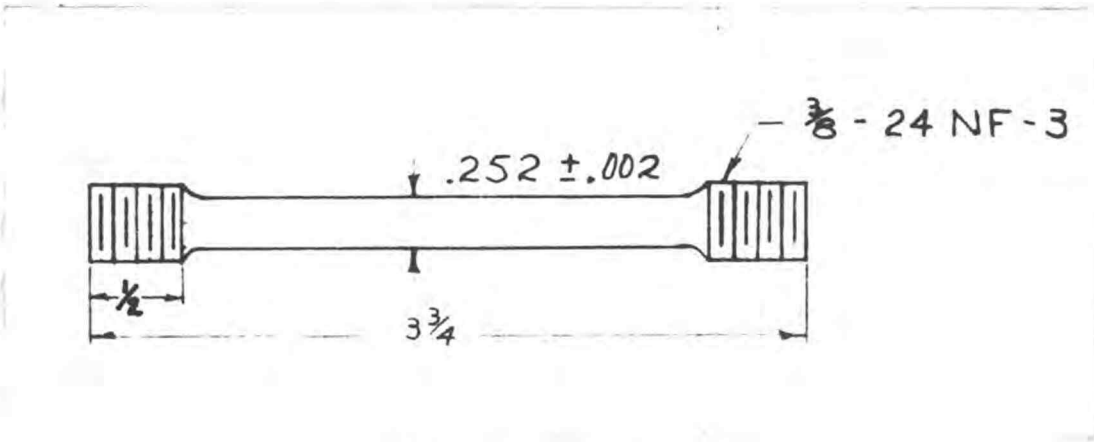

Figure 2 Specimen

All specimens were vacuum annealed for one hour at 750 C at 0.5μ Hg to give them a uniform texture or grain size and to relieve the cold worked condition of the surface . From x-ray diffraction techniques it was determined that each specimen was almost homogeneous throughout, but rod two had a slightly smaller grain size than rod three.

Temperature Measurements

Temperature measurement was made by means of copper-constantan thermocouples. Thermocouple potentials were measured using a No. 8662 Leeds and Northrup

potentiometer, with a reference junction of 32 F. A twelve point thermocouple switch was used to facilitate the reading of the thermocouple potential. The thermocouples were placed at the center and each end of each specimen and for each testing machine there were three wells, each well holding one specimen. Each machine then had nine thermocouples plus a reference junction.

Thermocouple calibrations were accomplished using room temperature and the boiling point of water, and no corrections were needed.

The temperature gradient, when the tensile extension arms were present, was as much as six degrees along the specimen gage length and even greater when the extensometers were used. Most of the tests, however, were carried out with a gradient of less than five degrees. The temperature variation at one point during a 500 hour test was as much as ten degrees, and in a few instances higher, but most of the tests were within five degrees during the entire test. Table I gives both the average temperature for each thermocouple and the standard deviation based on the testing period.

Extensometers

Extensometers of the telescope tube type with a rack and pinion type dial gage were used to indicate the

strain. Figure 3 shows an extensometer similar to the ones used, but modifications were made on the extensometer grips. The dial gages were Tumico Model BL. 1, reading to 0.0001 inch. The outside consisted of type 304 stainless steel tubing of 0.250 inch outside diameter and 0.028 inch thickness. The inside tube was of 3/16 inch outside diameter aluminum tubing. The outer tube was threaded in the dial gage support and the inside tube was threaded to the bottom extensometer grip. The upper extensometer grip was fastened to the outer tube with 6-32 x 3/16 inch cup-point set screws. Extensometer grips were made from 1 1/8 x 1/2 inch square cold rolled steel, drilled on one end to fit the specimen and on the other to fit the outside of the extensometer, and 6-32 x 3/16 inch cone point set screws were used as the grip at the gage mark.

Creep Tension Assembly

In testing a specimen under tension, it is desirable to have an axially aligned load applied, or a bending moment will be present in addition to the tension.

The tension assembly mount, which was attached to the lever arm from the load, was designed to have a free swing. In addition to this, Heim Unibal spherical rod

end bearings, HFX-7G, with 7/16 inch -20 NF threads, were attached at the threaded ends of the specimen to assure axial alignment.

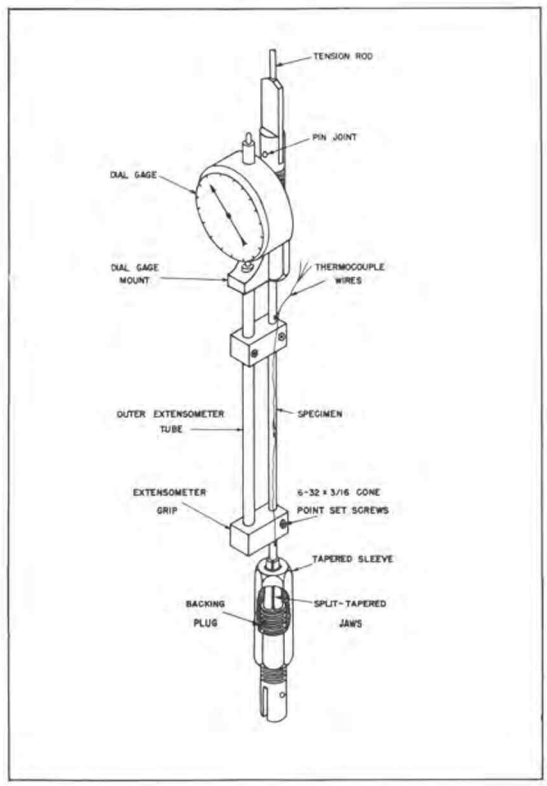

Figure 3 Extensometer

Attached to the ball joints were 16 x 7/32 x 1 inch extension arms with one end U-shaped to attach to the ball joint by a 3/8 NC bolt and at the other end with a 7/32 inch hole drilled to fit the tension assembly mounts at the top and the take up screw at the bottom. A 3/16 inch bolt was used to connect them. The U-shape was made

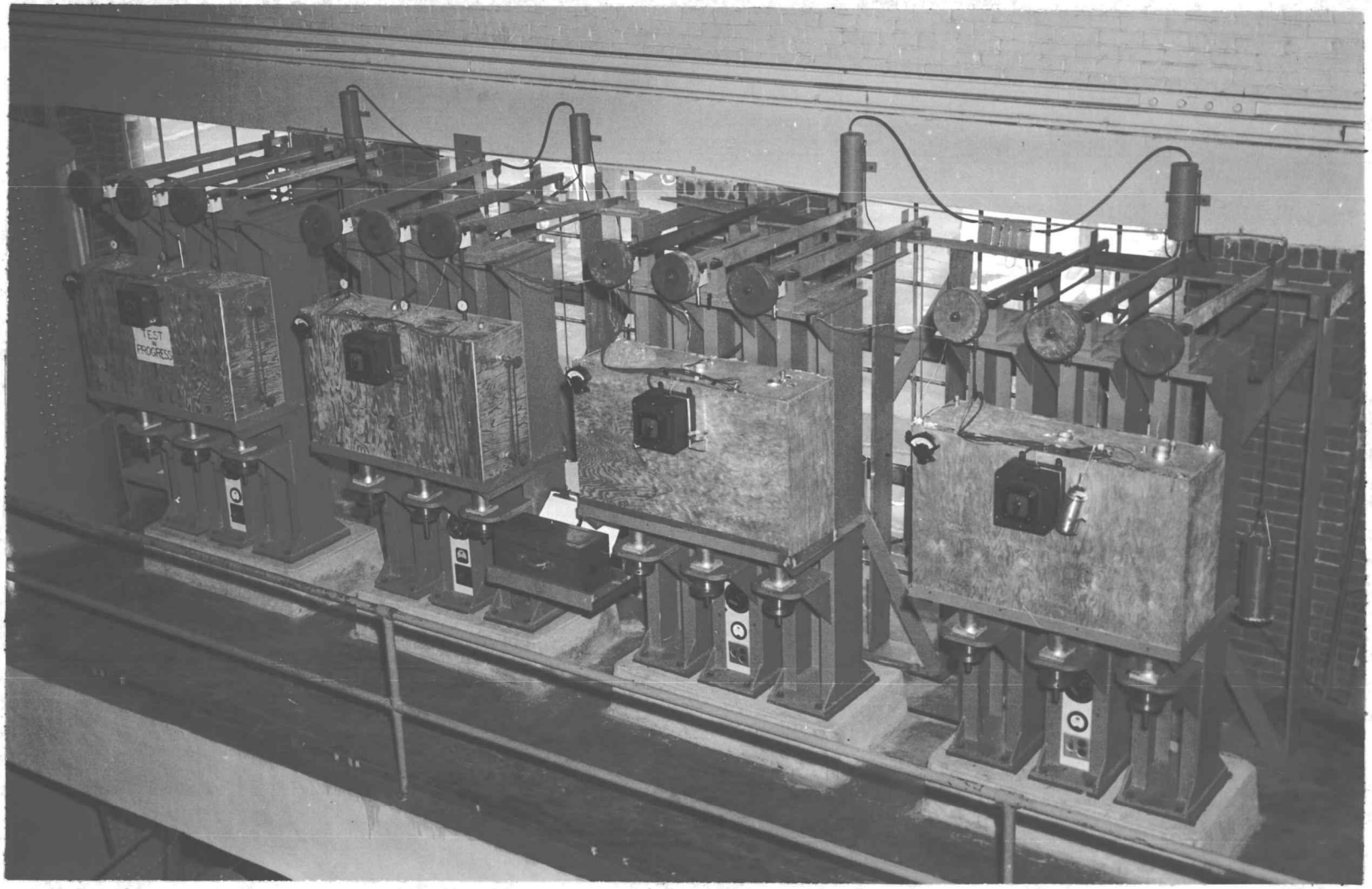

Figure 4 Creep Testing Machines

by welding three 1 1/2 x 3/16 x 1 inch pieces of cold rolled steel to the extension arm. Difficulty was encountered in using the ball joints, so a new design was tried which seemed to work satisfactorily. The new joints, 3/4 inch round rod 4 1/4 inch long, were threaded at one end to attach to the specimen and at the other end a 7/16 inch diameter hole was drilled perpendicular to the rod axis and then beveled and a curved surface machined so that it acted as a sort of a ball joint, this in turn attached to the extension arms with a 3/8 NC bolt.

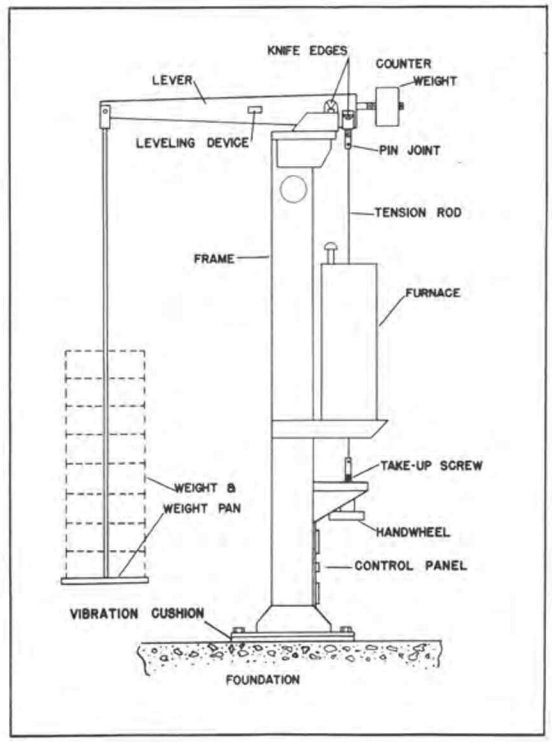

Figure 5 Testing Machine

Testing Machine

Two creep testing machines, described in detail elsewhere (6) and pictured in Fig. 4, were used in carrying out this research. Each machine consisted basically of a dead weight loading device, a boiling liquid furnace, and sufficient supporting structures to rigidly hold the specimen, furnace, and loading device (Fig. 5). Also, the testing machine supports were mounted on top of a vibration cushion to eliminate any vibration which might cause changes in the creep rate.

The boiling liquid furnace works on the principle that when a liquid is boiling it has a constant temperature and will remain at this constant temperature until all the liquid has completely evaporated. In using this type of furnace no regulating equipment is necessary.

It was desired to test zirconium at 500 F and a liquid had to be found which had a boiling point of 500 F. Dowtherm A, a eutectic mixture containing 26.5 percent dephenyl and 73.5 percent diphenyloxide, has a boiling point of 495.8 F and was selected because it is stable and has nearly the desired boiling point. One undesirable characteristic of Dowtherm is its low surface tension of 43 dynes/cm at 25 C; joints and valves must be sealed very tightly to contain it.

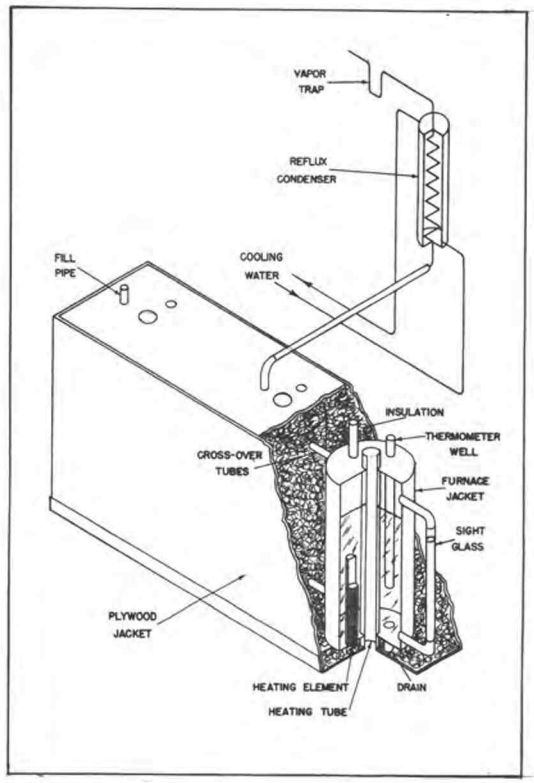

Figure 6 Furnace

Fig. 6 is a picture of the furnaces used. These furnaces consisted of an outer shell of 8 inch steel pipe and 1 1/2 inch pipe concentrically aligned with the outer shell to serve as the specimen's heating well. End plates were welded to the ends of the 8 inch pipe, not covering the 1 1/2 inch pipe. A heater well of 1 inch pipe and a drain pipe tube were on the bottom of the furnace. A set of three of these units was encased in a plywood jacket and fiberglass was packed loosely about each unit.

A 750 watt chromalox cartridge heater was used for each furnace and was more than sufficient to maintain the desired temperature. A sight glass was placed at the left of each set of three furnaces and all furnaces were connected on the bottom and top by 1/2 inch copper tubing. The center unit was attached to a 3/4 inch copper tube which was connected to a small reflux condenser to condense the vapor coming from the three furnaces. A gravity return system from the condensers was used; the condenser jacket was fabricated from 4 inch boiler tubing, with a helical coil 3 inches in diameter formed from lengths of 3/8 inch copper tubing. The condenser had a parallel flow system.

Load Calibration

The loads for the different specimens were determined by using a Baldwin U-1C load cell which measured the load with a sensitivity of 1.2 pounds. Since many different loadings were used, calibration charts for the different loading units were utilized. These were checked with the load cell and were within 1.2 pounds of the values given by the charts. The charts were a result of previous calibrations by dead weights.

Experimental Procedure

After receiving the specimens, a two inch gage

length was marked on each specimen with a Baldwin gage marker. Copper vs. constantan thermocouples were then attached at the two ends and middle of the specimen with copper wire. Because the furnace walls were not at a higher temperature than the specimen, it was unnecessary to shield the thermocouples. After the extensometers were attached, the specimens were put into the furnaces, which had been preheated to the testing temperature, and remained there for approximately two hours, until they achieved the testing temperature, before they were loaded.

The temperature readings were made five or six times a day until it was found that the temperature did not fluctuate beyond the ordinary limits of five degrees during the day. Thereafter temperature readings were made about once a day and sometimes only about four times a week. Temperatures were checked at night when the room temperature dropped and also on the weekend when the room temperature also dropped below average. It was found that this had some effect but was negligible compared to other factors which will be discussed later.

The extensometers were not used on the first group of five specimens but were employed thereafter. Due to sticking difficulties, strain data were very limited. It was noticed that after attaching the extensometers a marked temperature drop of about ten degrees from the

regular testing temperature was recorded.

Upon completion of testing and after removal from the furnaces, the specimens were placed in a refrigerator to avoid any recovery which might occur at room temperature. X-ray diffraction photographs were taken of each specimen before and after creep testing. Tensile and diffraction tests were conducted after the completion of the creep tests.

Discussion of Creep Test Equipment

The basic machine was designed to be operated at about 300 F yet seemed to handle the increased temperature sufficiently after new and larger heating units were installed. However, the heat transfer for temperatures at 500 F or above may be a little greater than is desired with the present design, and difficulty was encountered when the 750 watt heaters were installed because the base support for loading did not allow enough clearance to insert the longer 750 watt elements.

Difficulty was also encountered when unloading a specimen, especially one with a large load, because the load would tend to vibrate or oscillate, when turning the take-up screw, and set up very large impact loads on the specimen, which was undesirable.

As mentioned before, the heating fluid, Dowtherm, was very hard to contain; it has a very low surface

tension and will seep through the smallest opening. In the No. 4 testing machine leakage was a big problem. When the Dowtherm was heated so that it was vaporizing in large quantities, difficulty was encountered because returning fluid from the condenser tended to plug the outlet for the vapor and pressure pulses within the furnaces were set up. It was also found that if large quantities of fluid returned from the condenser it tended to lower the temperature in the center furnace as much as 15 degrees, whereas it had no noticeable effects on the end furnaces. The circulation of the Dowtherm from one furnace to the next did not seem sufficient to equalize the temperature in all three of the furnaces. The power-stat setting was very sensitive to this type of action.

The leakage of Dowtherm was also responsible for the burning out of two heaters. To counteract this, elements which had been hermetically sealed were ordered, but these were never used because no more failures were encountered.

The tension assembly was almost fully responsible for the temperature gradient along the specimens. This was determined when a specimen was run at no load and was suspended by a thin copper wire in the furnace. With this set-up the observed temperatures along the specimens showed no temperature gradient whatsoever. It was also found that if the thermocouples were not fastened

securely to the specimens but were off the surface any amount at all there was a great lowering of temperature. It is, therefore, suspected that the temperatures along the specimens were actually much closer than is shown by the temperature data.

The extensometer design for this test was not very satisfactory. Because of too much freedom in the tubing and the small two inch gage length, the results of the extension measurements were not very good.

Conclusions and Recommendations (Testing Equipment)

From the above discussion, certain conclusions and recommendations can be made:

1. For test temperatures higher than 300 F a larger unit with thicker insulation should be used to eliminate excessive heat transfer.
2. A modification of the heater well and/or the base support should be made to accommodate larger heaters, and a little better system of wiring should be designed. Internal wiring could be installed so that the heaters could be plugged in and easily exchanged whenever necessary.
3. The creep testing machine joints should be so designed as to accommodate any type of fluid.
4. Larger tubing between furnaces should be used

to better circulation, which in turn would give a more uniform temperature throughout. This would depend a certain amount on the type of fluid used.

5. A separate exit and return for vapor and condensate should be installed to eliminate pressure pulses, which accounts for some temperature fluctuation.
6. Hermetically sealed heaters should be used, and some type of heating jacket should be designed to put the heater in contact with the furnace wall.
7. Tension assemblies should be designed to have a minimum cross-section to decrease heat transfer.
8. A better type of extensometer system for specimen with small gage length should be found. It should be kept in mind that extensometers add to the heat transfer and should, therefore, be such as to give a minimum amount of heat transfer.
9. Prior to removing the specimens from the furnace, the furnace should be cooled, and then the load removed. This would eliminate any probability of recovery taking place between unloading and removal of the specimen from the furnace.

TABLE I INITIAL DATA ON CREEP SPECIMENS

Specimen Number	Stress (psi)	Well Number	Test Time (hours)	Average Temp.F Thermocouple #1	#2	#3	Standard Deviation in Temp.F	Max.-Min. Temp. F	Length (cm)	Average Diameter (inches)
3A	18,650	3L	500	494	494	490	0.75	488-494	5.08	.251
3B	25,000	3C	*Fra.-11						5.05	.2535
4C	35,000	4L	Fra. Loading						5.05	.252
4D	40,000	4C	Fra. Loading						5.08	.252
4E	22,000	4L	395	488	490	485	1.5	483-491	5.1	.2525
4F	22,000	4C	395	460	453	440	2	436-462	5.08	.253
3G	20,000	3C	395	495	496	488	1	488-498	5.08	.253
3H	18,650	3L	300	494	492	488	0.5	487-494	5.08	.252
3I	23,000	3L	Fra. 92-147	486	486	480	2	477-490	5.08	.252
3J	24,000	3C	Fra. 24-28	488	485	478	4	468-496	5.09	.252
4K	19,000	4L	501	488	488	484	2	480-492	5.08	.2525
4L	21,000	4C	501		471	477	10	454-490	5.09	.2525
3M	22,000	3L	501	488	487	486	2	478-490	5.09	.252
3N	20,000	3C	501	496	485	488	1.5	480-497	5.09	.252
4O	no stress	4L	501	495	495	495	1	494-498	5.09	.252
4P	Ten.tested	4C	0						5.09	.252
4Q	Ten.tested	4R	0						5.09	.252
3R	15,000	3L	500	489	489	485	1	482-490	5.09	.252
3S3	22,500	3C	Fra.-10	492	490	484	2	482-494	5.09	.253
3T3	12,000	3L	500	493	493	490	4	480-500	5.09	.251
3U3	8,000	3C	500		496	490	2	488-506	5.09	.253
3W3	18,000	3L	500	487	486	479	5	467-494	5.09	.249
3X	Ten.tested								5.09	.254
3Y	Ten.tested								5.09	.250
3Z	Ten.tested								5.09	.251

*Fractured

TABLE II FINAL RESULTS OF CREEP & TENSILE TESTS

Specimen Number	Elastic Modulus (10^5psi)	Ultimate Strength (psi)	Yield Strength (psi)	Tensile Elongation (%)	Creep Elongation (%)	Total Elongation (%)	Final Diameter (inches)	A	n
3A	3.215	76,000	63,000	17.1	5.85	25.8	.246		
3B									
4C									
4D									
4E	3.07	72,600	62,200	18	8.6	28.2	.2475		
4F	3.21	73,800	60,300	15.15	11.35	28.2	.2405		
3G	3.24	74,600	60,200	15.6	5.47	21.9	.247		
3H	3.945	73,200	57,400	19.75	3.13	23.45	.2485		
3I									
3J				39.1	39.1	39.1		.075	.48
4K	3.32	75,000	58,300	20.85	2.73	24.3	.2485		
4L	2.72	75,600	61,300	16.9	9.0	27.4	.242	.035	.237
3M	2.91	77,600	62,000	13.75	10.94		.2405	.05	.248
3N	3.01	74,800	59,300	20.4	7.04	28.9	.243		
4O	3.7	74,000	47,700	23.9		23.9	.2525		
4P	3.53	71,500	48,500	24.25		24.25			
4Q	3.42	72,200	46,300	25.8		25.8			
3R	3.58	71,900	51,300	14.45	.391	14.85	.254		
3S3					28.1	28.1	.240		
3T3	3.63	71,100	52,600	14.45	1.17	15.62	.253		
3U3	3.51	70,300	47,300	18	0	18	.252		
3W3				14	2.347	16.4	.249	.0076	.03
3X	3.42	70,200	44,900	12.5		12.5			
3Y	3.52	70,400	42,600	11.72		11.72			
3Z	3.37		44,200	10.95		10.95			

The ultimate strength, yield strength determined by the 0.2 percent offset method, the elastic modulus, and the ductility were the properties evaluated besides some creep properties.

The Creep Curve

In this research, extensometers previously described were used to obtain strain-time curves for some of the specimens tested. Due to difficulties with the extensometers, only a very few curves were obtained. The curves when plotted on log-log paper are straight lines as can be seen in Fig. 7, and this leads to the general equation for the first and second stages of creep, as the third stage of creep deviates from a straight line. The equation is as follows: $\epsilon = AT^n$

A - constant
T - time
n - constant

When the log is taken of both sides of the equation, it can easily be seen that A is the intercept and n is the slope of the curve. Table II gives values for A and n as read from the curves (Fig. 7).

It is also interesting to note that for a particular time, say 100 hours, if strain is plotted as a function of stress on log-log coordinates, it is found to be a straight line, suggesting that the strain is related to

stress by the equation $\varepsilon = B\sigma^{m}$

It can be noticed from the curves that both the slope and the intercept increase with increasing stress.

Not enough data were obtained on the creep curves of the different specimens to relate strain or minimum creep rate to stress time effects on subgrain formation.

Creep Rupture

The initial creep tests terminated in failure of the specimens. The first two, 4C and 4D, were subjected to 35,000 psi and 40,000 psi and 490 F and broke immediately after loading. The third specimen was loaded to 25,000 psi and failed after 11 hours of creep. The fourth specimen, under a load of 24,000 psi, failed after 26 hours of creep, and the fifth failed after about 120 hours. Fig. 8, a curve of creep rupture vs. creep stress, decreases exponentially but is not well defined due to lack of experimental data. All of the above specimens were from the second rod.

A specimen from the third rod was tested at 22,500 psi and failed after 10 hours of creep. From this it may be concluded that because of the slightly larger grain size of Rod 3 the rupture strength is lowered, which corresponds to effects of grain size on strength found by Lustman and Kerze (19).

Testing Equipment (Mechanical Properties)

A 60,000 lb. Baldwin Hydraulic testing machine was used to tensile test all specimens. The stress-strain curve was determined by the use of a non-averaging contact extensometer connected to a Templin stress-strain recorder. All specimens were loaded at the same rate, which was low enough to stay within the limits of the stress-strain recorder. The tensile properties of zirconium, however, are only slightly affected by strain-rate changes of the order of 100 times and only slightly more affected by rate changes of the order of 10,000 times.

Results (Mechanical Properties)

Fig. 9 shows typical stress-strain curves for the annealed and crept conditions. The results of the mechanical properties of the crept specimens, in comparing different stresses and temperatures, were rather sporadic, but do show marked changes from the specimens in the annealed condition.

By looking at Table II it can be seen that in the annealed condition specimens 4P and 4Q show ultimate strengths of 71,000psi and 72,200 psi and yield points of 48,500 psi and 46,300 psi. Specimen 3H on the other hand, which was under a creep stress of 18,650 psi for 300 hours and had the lowest creep strain, had an ultimate strength

of 73,200 psi and yield point of 57,400 psi. All specimens subjected to creep showed a three per cent or greater increase in ultimate strength and a 20 per cent or greater increase in yield point strength. A 10 per cent or greater decrease was noticed in the elastic modulus after creep, and it was found that the stress-strain curve of a crept specimen had no proportional section, but continually decreased in slope as the load was applied. An average of the maximum and minimum was used to evaluate the elastic modulus. It was also found that specimens which had been under greater creep stress and had the greatest permanent deformation also had the greatest variation in elastic modulus as the stress was increased.

To have a true measure of the effects of creep on the mechanical properties as compared to room temperature permanent strain, some tests should have been made on room temperature specimens which had been cold worked the same amounts as the specimens subjected to creep.

The ductility of the specimens subjected to creep decreased, but considering the total strain, both that due to creep and that due to tensile testing, it was found that the elongation was about the same as that of specimens in the annealed condition.

All fractures were of the irregular fibrous type.

Discussion of Results (Mechanical Properties)

The effects of creep have been found in this research to increase the room temperature yield strength and ultimate strength and to decrease the ductility of zirconium. Similar effects are encountered in metals which have been cold worked to varying degrees. It has also been found that the strength of a metal increases when the grain size decreases; it was noted in x-ray analysis that both strain hardening and a subgrain formation were present within a specimen due to creep conditions, and this may be the explanation for the increase in strength and decrease in ductility.

Work done by Gluck, Voorltees, and Freeman (12) in determining effects of prior creep on the mechanical properties of aluminum and stainless steel, has shown that the effects of creep lower the yield strength and ductility. They were working, however, at very low strain rates and percentages of deformation which would increase the probability of error due to inhomogeneous materials.

Other work, done by Wilder, Ketterer, and Collyer (26), on carbon and low alloy steels at 900 F and 1050 F, showed that the yield and tensile strength were, in general, decreased after exposure for 10,000 hours, and the ductility was increased. However, in Tapsell's text, Creep of Metals (25), he introduces work done by several investigators without exception found that prior creep increased

the yield strength and ultimate strength and slightly decreased the ductility.

The above contradiction may be due to many effects. First, it may be that in all researches which found an increase in yield and ultimate strength and a decrease in ductility that strain hardening was taking place at a faster rate than recovery, and, as in ordinary strain hardening, the strength would be increased. In researches which found contradictory results, recovery may have been taking place faster than strain hardening, and this may lead to a decrease in strength and an increase in ductility. The annealing histories of the different metals would probably have some effect on this recovery-strain hardening phenomenon due to creep conditions. A second point of interest is that prior creep may have quite different effects on the mechanical properties depending on whether the creep is carried out above or below the high temperature yield strength of the metal.

The stress-strain curve of the creep specimen showed continual curvature during load. This is similar to imperfect elastic materials such as concrete and cast iron, and is also characteristic of a large number of metals having prior strain hardening. This phenomenon is not fully understood.

It is recommended that further study of the effects

of creep on the mechanical properties be made. Many investigators have found that of all the mechanical properties tested, which included hardness and tensile properties, that notch impact strength is most affected by creep. No notch impact tests were conducted on zirconium used in this research.

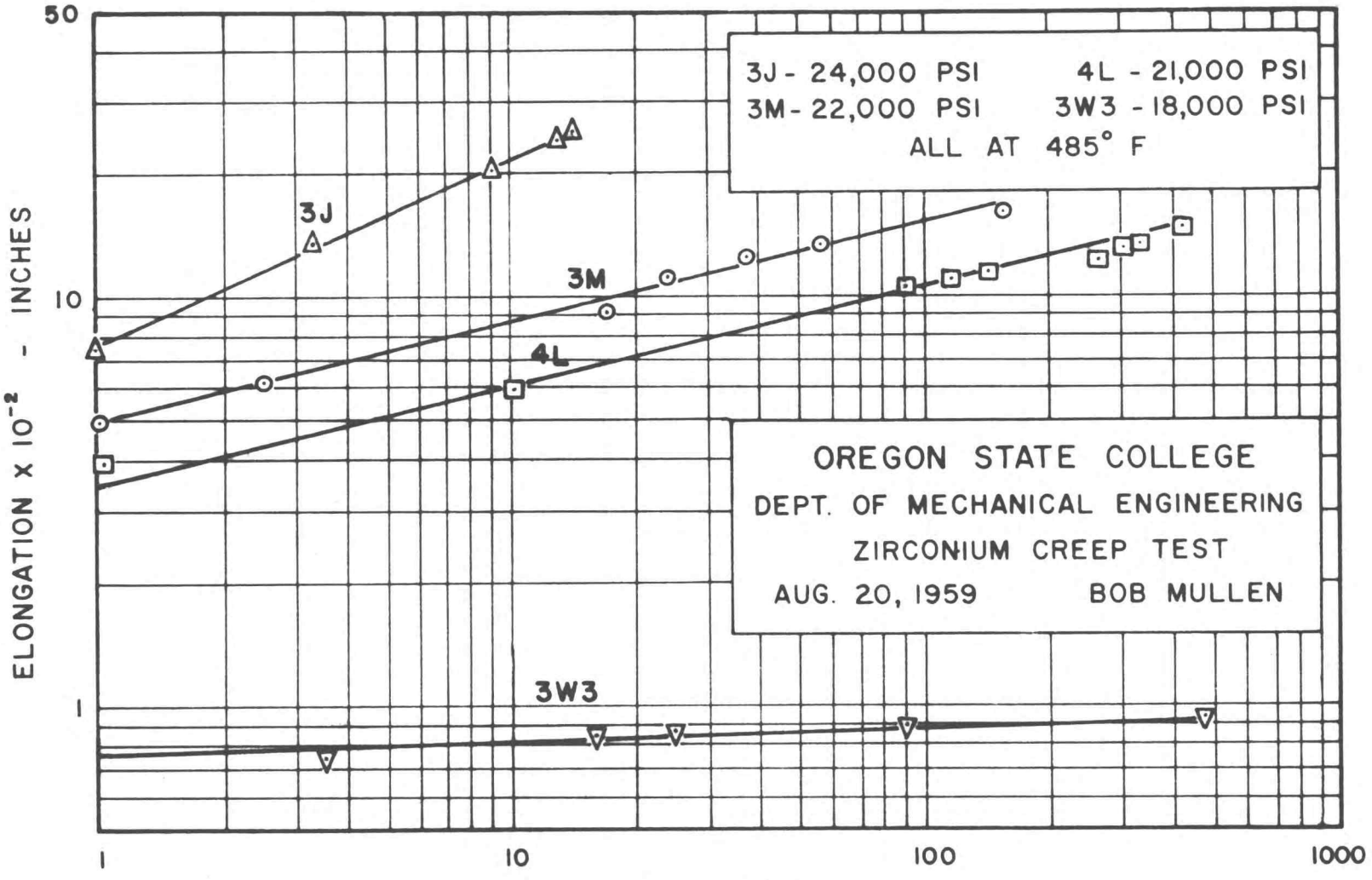
50
10
1
ELONGATION X 10^{-2} - INCHES
3J - 24,000 PSI
3M - 22,000 PSI
4L - 21,000 PSI
3W3 - 18,000 PSI
ALL AT 485° F
3J
3M
4L
3W3
OREGON STATE COLLEGE
DEPT. OF MECHANICAL ENGINEERING
ZIRCONIUM CREEP TEST
AUG. 20, 1959
BOB MULLEN
1
10
100
1000
TIME - HOURS

FIGURE 7

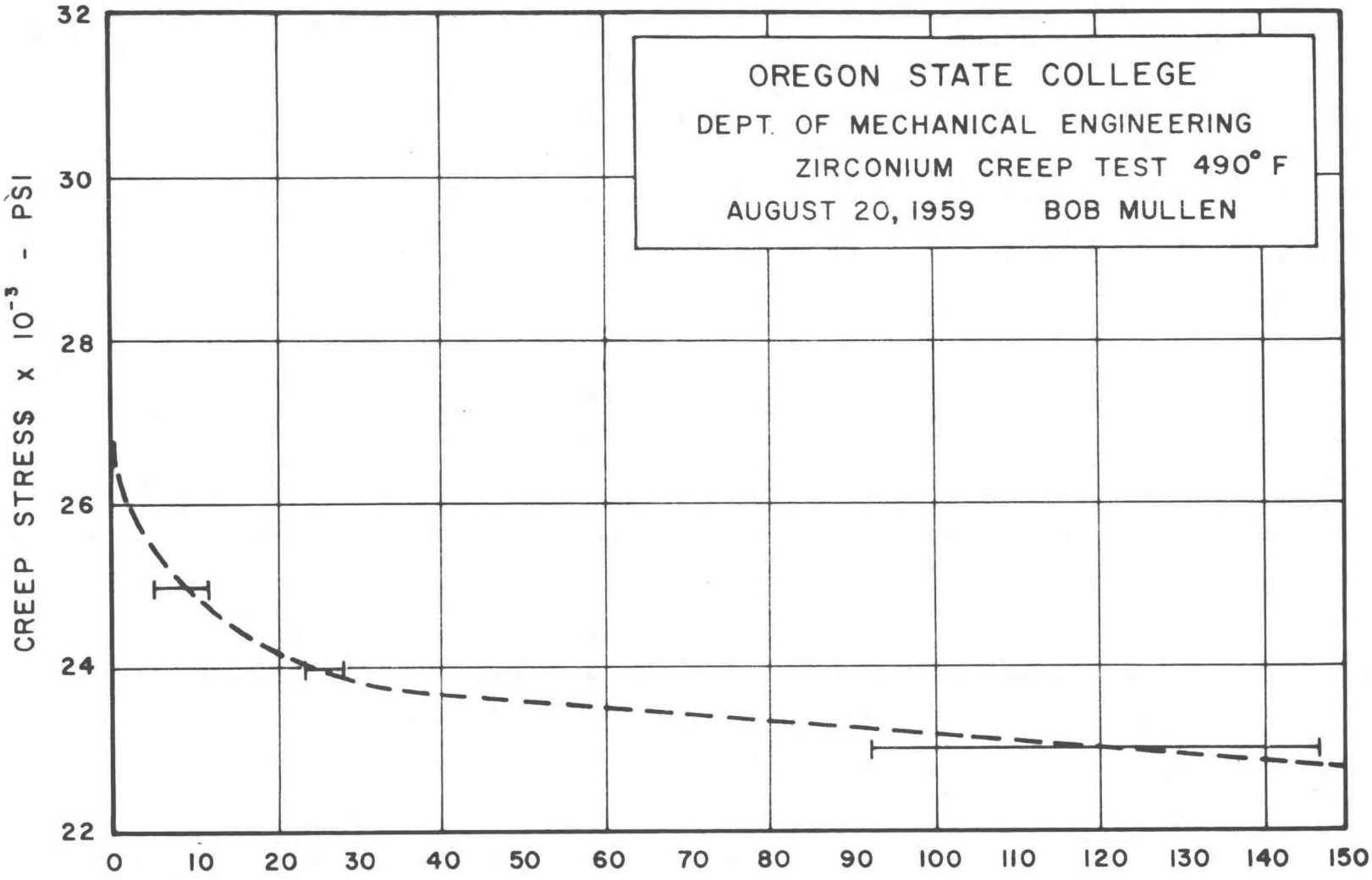
OREGON STATE COLLEGE
DEPT. OF MECHANICAL ENGINEERING
ZIRCONIUM CREEP TEST 490° F
AUGUST 20, 1959 BOB MULLEN
CREEP STRESS x 10^{-3} - PSI
32
30
28
26
24
22
0
10
20
30
40
50
60
70
80
90
100
110
120
130
140
150
TIME TO RUPTURE - HOURS

FIGURE 8

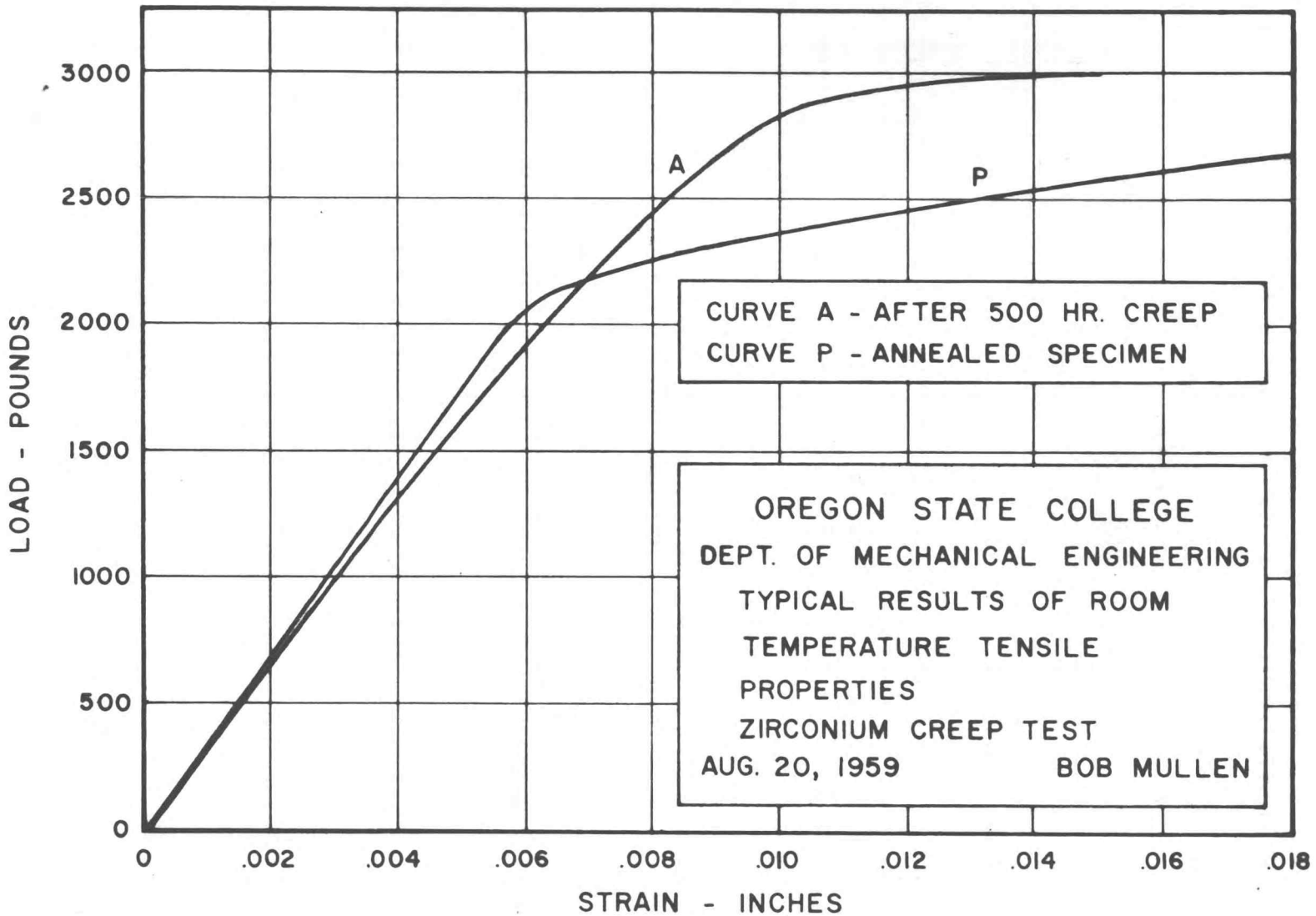
LOAD - POUNDS
3000
2500
2000
1500
1000
500
0
0
.002
.004
.006
.008
.010
.012
.014
.016
.018
STRAIN - INCHES
A
P
CURVE A - AFTER 500 HR. CREEP
CURVE P - ANNEALED SPECIMEN
OREGON STATE COLLEGE
DEPT. OF MECHANICAL ENGINEERING
TYPICAL RESULTS OF ROOM
TEMPERATURE TENSILE
PROPERTIES
ZIRCONIUM CREEP TEST
AUG. 20, 1959
BOB MULLEN

FIGURE 9

X-RAY DIFFRACTION

Theory and Procedure

In determining changes of structure of zirconium after being subjected to creep, x-ray diffraction was used.

X-ray diffraction can indirectly reveal details of internal structure of the order of 10^{-8} cm in size. It is, therefore, profitable to elucidate the effects of structure on x-ray patterns and the basic reason for them.

X-rays are electromagnetic radiation of exactly the same nature as light but of a different wave length. The wave length range is from about 0.5 to 2.5 angstroms. The x-rays follow the laws of wave propagation and diffraction and also act as discrete particles possessing a definite energy and momentum.

X-rays are produced by accelerating particles, usually electrons, by a high voltage source and bombarding a metal target with these electrons. Continuous or white radiation originates when the electron encounters an electron in the target. It may convert all of its kinetic energy into x-rays at a single encounter but more than likely the electron's energy will be dissipated through a series of glancing blows with many different electrons in the target material, consequently giving many different wave lengths of radiation. If the electron makes a direct

hit on an electron within the target metal, and it has sufficient energy, it will knock the electron out of its atom. Then when an electron from an outer shell jumps into the vacated position at a lower energy level it will emit energy as radiation. This radiation is characteristic radiation since the transition from one energy level to another involves a definite amount of energy. Using different targets, different wave lengths of radiation may be obtained. Each target emits characteristic radiation, if the voltage is sufficient, besides the white radiation. The characteristic radiation is essentially of one wave length and has usually a much higher intensity, therefore having more effect on a photographic plate.

The radiation thus being emitted by the target is passed through a collimator and a fine beam of x-rays is directed on the specimen where it is diffracted and the diffraction recorded photographically. Sir William Bragg derived a simplified law for the requirements for a successful diffraction to occur. In order to have diffraction, which can be recorded, a number of diffracted waves must be in phase in order to reinforce each other. The picture below will help to show the relationship which Bragg derived.

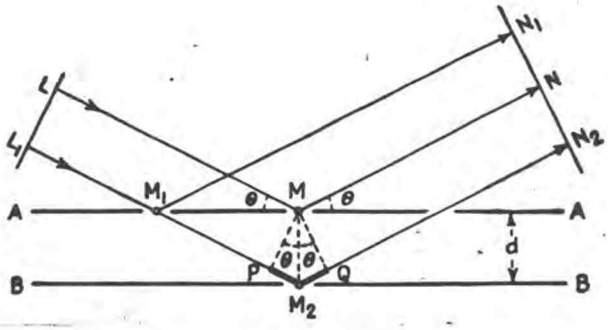

In order for the diffracted rays to be in phase

$n\lambda = 2d\sin\theta$

λ = wavelength

Figure 10

Now for a given wave length and a 'd' spacing between two planes, there is only one angle which will satisfy Bragg's equation. For a polycrystalline substance there are enough crystals randomly oriented to supply a given set of planes, having a certain 'd' spacing with the appropriate angle for diffraction, whereas with a single crystal, unless it is rotated, there is little chance for diffraction to occur with a random setting of the crystal.

Considering a three-dimensional picture of a polycrystalline material, it can be seen that because of the random orientation of the grains of an annealed metal, diffraction will satisfy Bragg's law and will diffract at equal angles but in different directions for many crystals and will, therefore, describe a cone of radiation being diffracted from a particular plane of all the crystals, as shown in Fig. 11.

A photographic plate placed, therefore, in a position to record the diffractions, will record circles or arcs depending on its position and size.

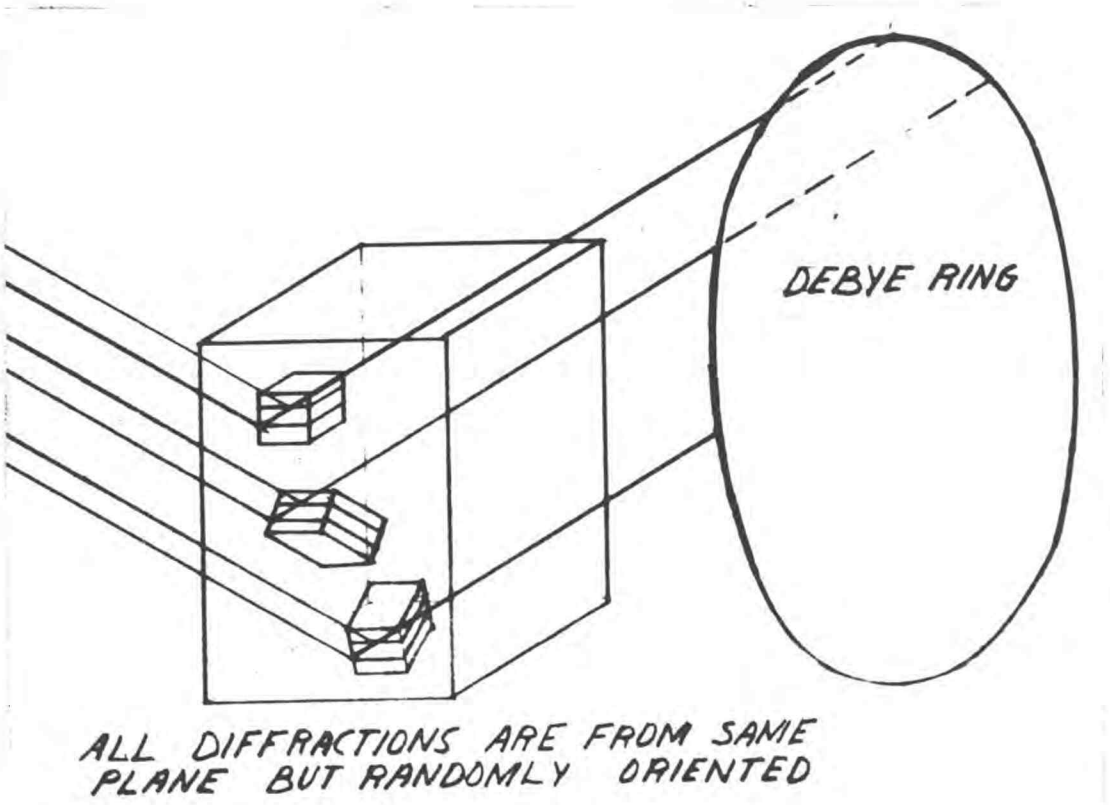

Figure 11 Diffraction Pattern

From the photographic plate a number of conclusions may be determined from the characteristics of the diffractions pattern.

First, if the material has a large grain size there will not be as many diffractions in different directions with equal angles and the pattern will have a spotty consistency. The grain size of commercial metals and alloys range from about 10^{-1} cm to 10^{-4} cm.

As the grain size decreases, more crystal grains will be diffracting and the spotty consistency will change to a more uniform circle called a Debye ring. When the

grain size reaches a value somewhere in the range of 10^{-3} to 10^{-4} cm, the Debye rings lose their spotty character and become continuous. Between this value and 10^{-5} cm, no change occurs in the diffracting pattern. At about 10^{-5} cm the first signs of line broadening, due to small crystal size, begin to be detectable.

Second, the crystal perfection may be determined. The effect of strain, both uniform and non-uniform, on the direction of x-ray diffraction is illustrated in Fig. 12 below.

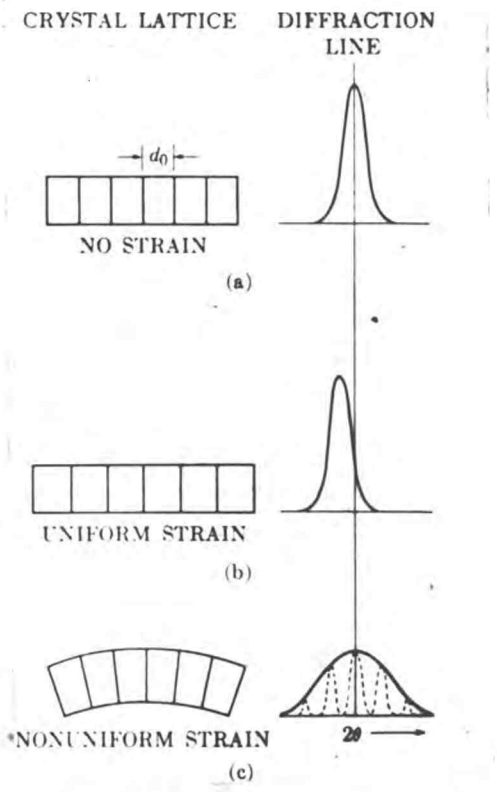

Figure 12 Effect of lattice strain on Debye-line width and position (8).

It has been well established that the effect of cold work is to broaden the Debye rings but the explanation of this is under some controversy. Some investigators have felt that the chief effect of cold work is to fragment the grains to a point where their small size alone is sufficient to account for all of the observed broadenings, whereas others feel that the non-uniform strain causes most of the line broadening except for a small part due to fragmentation.

Third, preferred orientation may be detected by the grouping of the diffraction pattern in certain directions as previously explained. In other words, the grains would not have a random orientation but would be aligned in only certain directions and this would create only partial Debye rings or arcs of Debye rings.

X-ray Procedure

In this research, because of the limited number of specimens, the back reflection technique of x-ray diffraction was almost entirely used. This technique enables one to use a large specimen for diffraction purposes. Copper radiation, which gives characteristic radiation of two wave lengths, $K\alpha_1$ and $K\alpha_2$, is usually used with the $K\beta$ filtered out with a nickel filter. After taking many pictures of this type and others without the nickel filter

it was decided that the unfiltered radiation would be used because it decreased the exposure time from five to three hours and also in comparing the specimens subjected to creep with those in the annealed condition, it was advantageous to have as many diffraction lines or Debye rings as possible to get a better comparison.

After being annealed and also after being subjected to creep for 500 hours, a thin film of oxide was present on the specimens. A back reflection photograph is representative of only a thin surface layer of the specimen. It was, therefore, necessary to check to see if the oxide layer was thick enough to have an effect on the pattern. Most of the specimens were etched and it was found that there was no noticeable effect from the oxide layer. However, all specimens were etched before x-ray exposure.

The developing procedures for exposed x-ray film and x-ray exposure were standardized so no erroneous comparisons would be made. An x-ray exposure time of three hours was finally arrived at as the best, for minimum exposure and maximum intensity.

Results

From the back reflection x-ray photographs it was found that the grains of rod two were uniform throughout the entire rod. The grain size was approximately 1.17×10^{-2} cm in the annealed condition. In the third rod the

grain size was a little larger than the second, 1.3 x 10^{-2} cm, but was again uniform throughout the rod.

Fig. 13 and 14 show a comparison of the back reflection x-ray pattern before and after anneal. Fig. 13 shows very broad, smooth Debye rings which are characteristic of a cold worked material due to the non-uniform stress and fragmentation of the grains. Fig. 14 shows the annealed condition where the grains are very large and stress free.

After subjecting specimen 3A to 500 hours of creep at 18,650 psi and 490 F temperature, the x-ray pattern Fig. 15 shows the Debye rings have started to form more clearly than in the annealed specimens and the $K\alpha_1$-$K\alpha_2$ doublet is separated. Specimen 3A shows a subgrain formation as can be seen from the much greater frequency of spots, and it reveals some line broadening which indicates a limited amount of cold work or non-uniform stress. Fig. 16 is specimen 3H which was under the same conditions as 3A but was only exposed to creep for 300 hours instead of 500 hours. 3H does not have as many subgrain formations and shows no appreciable non-uniform strain or cold work. The $K\alpha_1$-$K\alpha_2$ doublet is very distinct.

In comparing Fig. 17 and 18 where both specimens were under identical loads and times of exposure but 4E had a test temperature of 489 F and 4F had a temperature of 450 F, it may be seen that they are almost identical as far as grain size and amounts of cold work except that 4F may have

a little more observable cold working. This would indicate that the crystals are insensitive to difference of temperature as high as 40 degrees at 450 F. This may be explained, though, in the fact that at this particular grain size, 10^{-3} to 10^{-5} cm, x-ray diffraction is very insensitive to changes and would, therefore, presumably not show any change.

Comparing Fig. 19 and 20, where the specimens were under two different stresses, 4L at 21,000 and 4K at 19,000 psi, and different temperatures also, it can be seen that there are marked differences between the two. We may conclude from this and the previous Fig. 17 and 18 that the difference is caused entirely by the difference in stress. One item which must be mentioned, however, about Fig. 19 and 20 is that neither specimen was in the insensitivity region of grain size determination that Fig. 17 and 18 were. Supposing that there were differences in Fig. 17 and 18 due to temperature which could not be noticed because of the insensitivity, it is very likely that the differences in Fig. 19 and 20 are from temperature differences as well as stress, but from indications from other specimens tested, the above is not true and temperature effect is much less noticeable than stress and time effects.

So far none of the specimens in Fig. 13 - 20, it should be noticed, have shown much sign of preferred orientation.

It was deemed advisable to check the effects of temperature alone, and Fig. 21 is a diffraction pattern of specimen 40 which was subjected to 495 F for 500 hours under no stress. In comparing it with Fig. 14, they are almost identical and it may be concluded that temperature alone in the range investigated has no effect on the grain size or crystal perfection.

Fig. 22 and 23 are specimens 3G and 3N. Both were under identical conditions of stress, temperature, and time, and no noticeable differences were observed in them. Also diffraction pictures of the same specimen, only in a different position, were taken and no change from one position to the next was noticed. This would tend to verify the fact that each x-ray diffraction picture was representative of the whole specimen and local effects were not being recorded.

Fig. 24 and 25 are diffraction pictures of specimens which fractured; the first after 26 hours at 24,000 psi and the second after 120 hours at 23,000 psi. They both show fine grain size or subgrain formation to a very high degree and some cold work, but the $K\alpha_1$-$K\alpha_2$ doublet is still discernable, which indicates that there are no excessive amounts of cold work, such as is found in Fig. 13 after machining.

Two specimens broke almost instantaneously after loading, and their patterns show a greater amount of line

broadening than Fig. 24 and 25.

Fig. 26 is a diffraction photograph of specimen 4Q, which was not subjected to creep, after it had been fractured in tensile testing to determine its mechanical properties. In comparing this with Fig. 27, specimen 3J, which broke after 26 hours under creep conditions, it is noticed that specimen 4Q has much greater line broadening than 3J.

Fig. 28 is a diffraction picture of a specimen which had not been subjected to creep, but was deformed 4 per cent at room temperature. It is very clear from this that the specimens subjected to creep conditions are undergoing a different process or mechanism of deformation than are specimens under ordinary conditions.

The Debye rings pictured in all back reflection figures are, from the outside toward the middle; first, the 006 planes; second, the 205 planes due to $K\beta$ radiation; third, the more distinct doublet from the 205 planes due to $K\alpha_1$ and $K\alpha_2$ radiation; fourth, the 214 planes, also from $K\alpha_1$ and $K\alpha_2$ radiation. The next more faint doublet is the 220 planes due to $K\alpha_1$ and $K\alpha_2$ radiation. The two inside rings are due to $K\beta$ radiation and were not identified.

None of the above planes are related to the family of planes which take part in slip, namely the (001) plane, or the (100) direction, of close-packed hexagonal zirconium.

Before going into the discussion of the results of

this x-ray diffraction data, it will be necessary to discuss the processes of recovery, recrystallization, and grain growth. When a cold worked metal is heated to a certain temperature, depending on the amount of cold work and type of metal, a process of stress relief starts to take place and is called recovery. The recovery process is undetectable metallographically, but is characterized by a line sharpening of the x-ray diffraction pattern.

At a high temperature, again depending upon the amount of cold work, primary recrystallization begins and when completed, the disturbance or internal strain is almost completely removed. Primary recrystallization takes place by growth from nuclei to form an entirely new structure.

Grain growth follows primary recrystallization and occurs only at a higher temperature than either recovery or primary recrystallization. It is characterized by a uniform coarsening of the structure, involving a reduction in the number of grains.

Secondary recrystallization takes place after grain growth only when the material has been severely cold worked and primary recrystallization did not completely eliminate the internal strain.

A structural change has recently been recorded by x-rays after a deformed specimen has been annealed, in

which the relation of the new structure to the old is much closer than is usual in primary recrystallization. This structural change was first called, by some investigators, recrystallization in situ, but was later given the name polygonization. It is characterized by an asterism of a Laue photograph being separated into many spots but remaining in the same position as the original parent asterism. It can be seen in terms of dislocations by the figure below. 'a' is the randomly oriented dislocations and 'b' the crystal in the polygonized state with the dislocations in line. The difference between recovery and polygonization is not very well defined but they are believed to be separate processes.

The minimum recrystallization temperature for zirconium is about 400 C but recovery has been found to occur at as low a temperature as 100 C. It is probable that in this research, recovery and polygonization may take place during creep, but it is unlikely that there will be any signs of recrystallization.

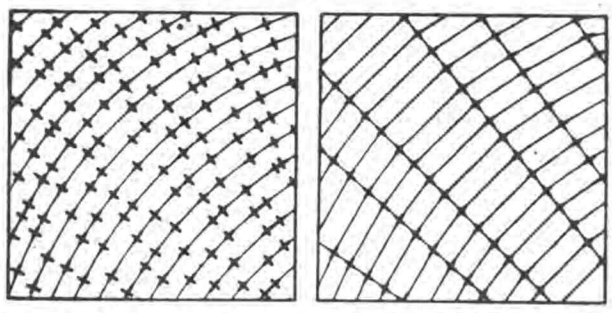

Ref. (13)

Discussion of Results (X-Ray Diffraction)

In comparing Figs. 15-28 with Fig. 14, it is evident that some type of subgrain growth or grain fragmentation is taking place.

Jenkins and Mellar (18),working on the creep of mild steel, have found metallographic evidence of a kind of substructure within the grains after deformation at high temperature. Homes (17), in using x-ray diffraction, has noticed after the deformation of steel at high temperature, that the original x-ray spots were sharply divided into several small ones. Hirst (16) has made the same observation with his work on lead and Crussard (7) from his work on aluminum.

The work done by the above men and this research demonstrates almost beyond any doubt that the splitting or dividing of x-ray spots is due to the division of grains into subgrains under load and temperature.

There are, essentially, two theories on the mechanism of deformation of the grains into subgrains; first, as summarized by Gervais, Norton and Grant (11) and based on the work on polygonization by Cahn, Guinier and Lacombe, Greenough and Smith, Crussard, Servi, Norton and Grant, it was concluded that the subgrain formation could be attributed to two simultaneous effects, inhomogeneous deformation which produced bending of the lattice and polygonization; second, work done by Wood and co-workers

developed a theory of fragmentation. Woods did not recognize polygonization as a fundamental mechanism and said that aluminum, at the beginning of deformation, immediately fragmented into subgrains to permit deformation of the metal. They reached the conclusion that deformation of grains occurred by flow along the subgrain boundaries.

The x-ray work of this research has shown two things as far as explaining a mechanism for subgrain formation; first, a striated structure was formed, Fig. 16, subsequent to creep and this striated structure can be explained in terms of the polygonization process discussed previously; second, from Figs. 26 and 27 and also Figs. 24 and 25, a line sharpening and intensity increase was observed on the crept specimen whereas broad lines were characteristic of room temperature loading. This would suggest that either some type of recovery process is going on during creep, which does not occur at room temperature, or, due to the creep conditions, the crystals do not undergo as much internal strain which would indicate that grain boundary slip was predominate. Evidence to support the recovery hypothesis, from work done by McGeary and Lustman (20), indicates that diffracted x-ray intensity and hardness of 97 percent cold rolled arc melted crystal bar zirconium underwent measureable changes at temperatures as low as 200 C and very substantial changes at 300 C.

Work done by Gervias, Norton and Grant (11) on

creep of coarse grained high purity aluminum at temperatures approaching the melting point led to two processes of subgrain formation; kinking and polygonization. Polygonization was considered as the main factor in subgrain formation.

Polygonization or recrystallization in situ have been found to occur in specimens subjected to creep at moderately high temperatures without the necessity of any subsequent annealing. These two processes are characterized by splitting of asterisms in a Laue photograph. This would be analogous with the splitting of one Debye ring into three or four concentric circles or the spotty character of a crystal which has been strained, as shown clearly in Fig. 16.

A recovery process as discussed before may be taking place besides the polygonization or in conjunction with it. It has been found from other experiments that if the temperature is high enough recovery occurs presumably throughout the crystal and this is followed, or rather accompanied, by polygonization which takes place in regions where the lattice is curved. There is as yet insufficient experimental evidence to decide how much of the change ascribed to recovery is in fact polygonization, but it is fairly certain that the two processes are distinct.

It has been found by Guinier (13) and Tennevin that even when both recovery and polygonization are complete

the effects of cold work have not been entirely removed. It was also found by these investigators that polygonization began at 320 C in the specimens (aluminum) elongated two per cent and at 280 C in those elongated five per cent. It was also found that in a polycrystal which was even more deformed it is probable that recrystallization takes place before any detectable polygonization has developed.

Since most specimens in this research underwent 15 per cent or more deformation, the above statement would tend to contradict previous evidence of polygonization but since the above evidence was obtained from aluminum samples, it would not necessarily hold for zirconium since zirconium has a higher melting point and therefore a high recrystallization temperature.

Recovery according to Burgers (13) is to be regarded as a rearrangement of the deformed lattice through the rearrangement of the dislocations present. McGeary and Lustman (20) have described recovery in terms of dislocation mechanisms of polygonization, in which edge types of dislocations perpendicular to curved slip planes accummulate during heating, leaving a multitude of minute stress free grains. In the case of zirconium, the above phenomenon first observed by x-ray diffraction is a gradual sharpening of the cold rolled texture. It was noted by Bostrom & Kulin (3) that the recovery process takes place

at comparatively low temperatures for such a refractory metal as zirconium. Some 25 per cent of the effects of cold working (97 per cent reduction in area) is relieved in about 300 minutes at 250 C which is below the temperature at which the present research was carried out.

A small or subgrain size was formed when a higher stress level or strain rate was used. This is also evidenced by Gervais, Norton, and Grant (11). They also found that subgrain size increased markedly with temperature at the high temperatures at which they were working, whereas in this research it was found that temperature had little effect as far as subgrain formation was concerned. Sherby and Dorn (22), in their attempt to correlate the creep properties of dilute alpha solid solutions in aluminum with the subgrain structures, however, found that the structure of fractured creep specimens appears to be a function of the creep stress independent of test temperature. In the present research it was also found that the subgrain formations were a function of stress and time but were independent of temperature.

The effects of creep on the lattice parameters of zirconium were determined by the use of the powder method. The lattice parameters were calculated for both the annealed condition and for a greatly cold worked specimen. The calculation of angles and 'd' spacing were made on a desk computer and no significant change of lattice

parameters has been noticed. In fact, the accuracy with which the lines can be measured and the angles and 'd' spacing calculated is insufficient to determine the effects of creep on the lattice parameter.

It can be noticed from the powder patterns, Fig. 30, that preferred orientation is observed on the low angle diffractions of the cold worked specimen but not at the high angle. This may be the reason why no preferred orientation was found on the back reflection pictures, their being high angle diffractions.

Summary of X-ray Discussion

1. A sub-structure caused by fragmentation of larger grains took place in the specimens subjected to creep, and changes of stress and time had marked effects on the subgrain structure. Increases in both stress and/or testing time decreased the subgrain size whereas no significant effects due to differences in temperature were noted.
2. The formation of the substructure was related to non-uniform stress and its relief by polygonization and recovery as shown in Fig. 16.
3. From ruptured specimens, one due to creep, the other due to tensile testing, it was concluded that the line sharpening in the diffraction pattern of the crept specimen was due to either a recovery process,

which can take place as verified by McGeary and Lustman, or under the creep conditions the specimen does not undergo as much internal deformation which suggests a grain boundary type of slip.

4. There were no noticeable changes in lattice parameters of 'd' spacing between planes due to creep. One difficulty in determining this is in accuracy of measurement and the other is differentiating between effects of line broadening due to fragmentation and those due to changes in 'd' spacing.

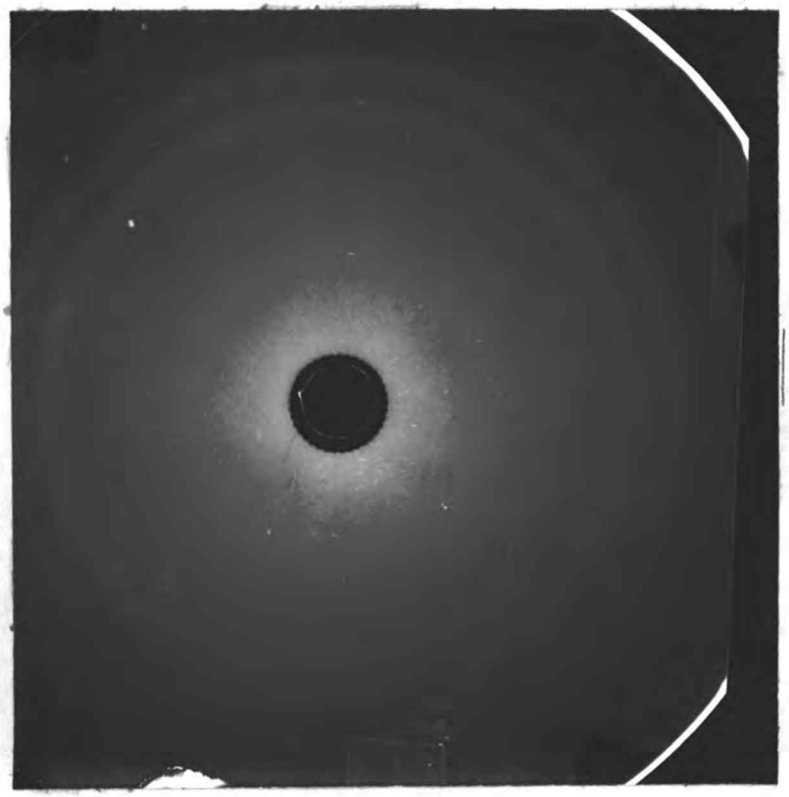

Figure 13

After machining before vacuum anneal

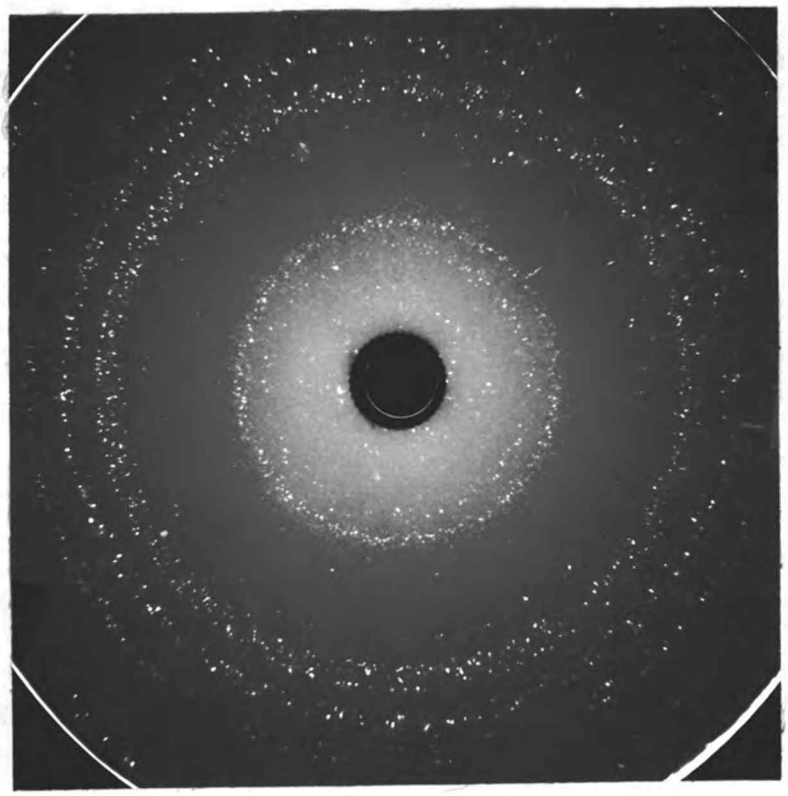

Figure 14

After vacuum anneal 750 C 1 hr.

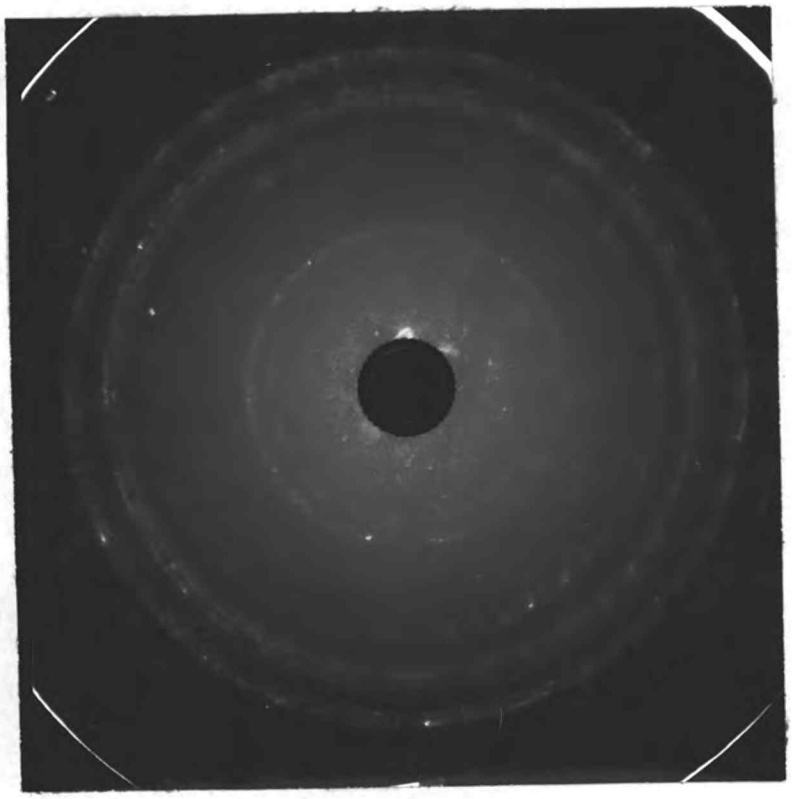

Figure 15

Specimen 3A
18,650 psi
at 490 F
500 hr.

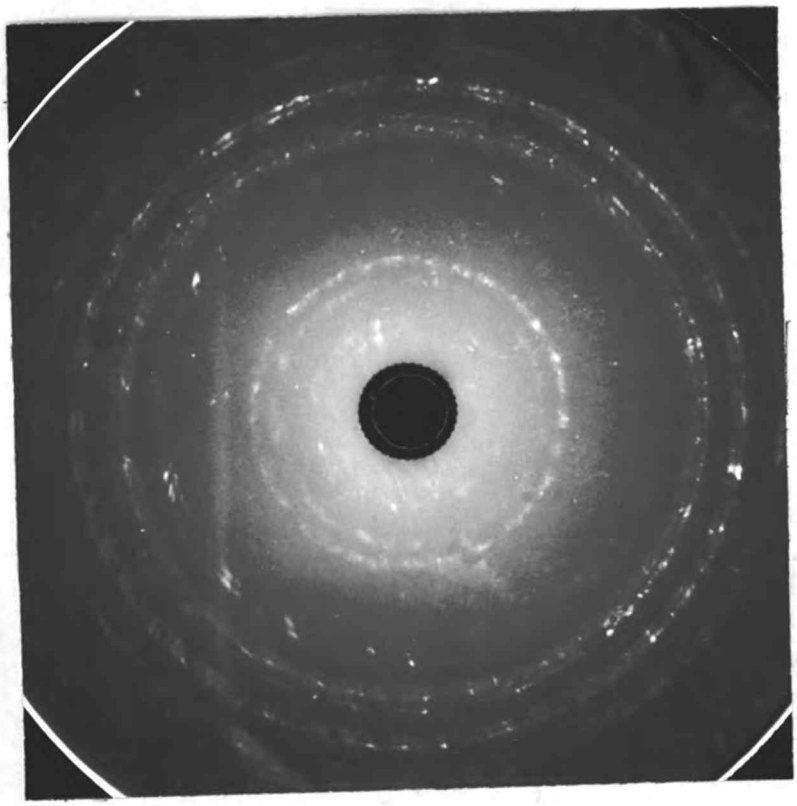

Figure 16

Specimen 3H
18,650 psi
at 490 F
300 hr.

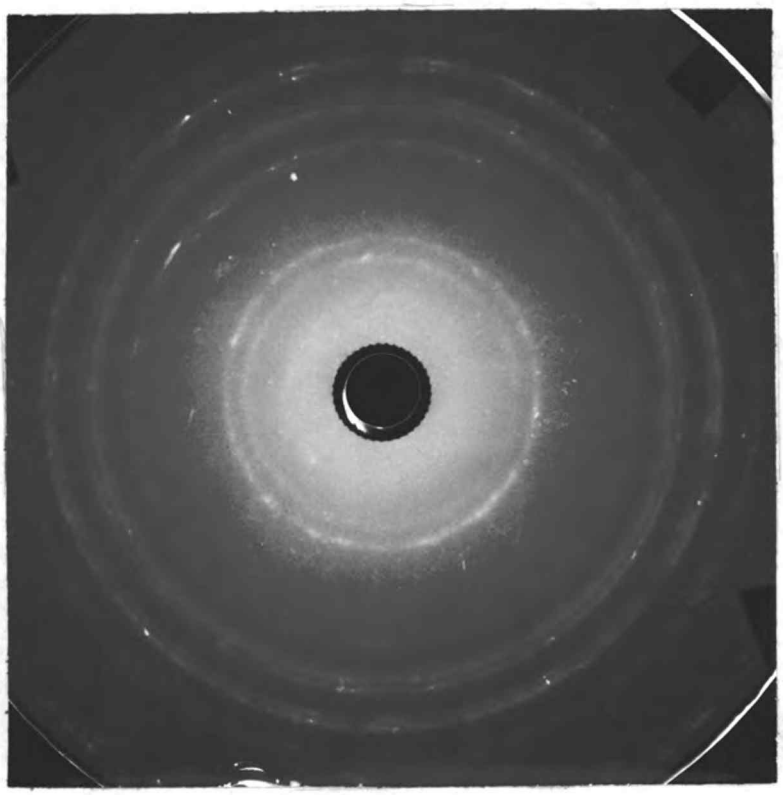

Figure 17

Specimen 4E
22,000 psi
at 489 F
395 hr.

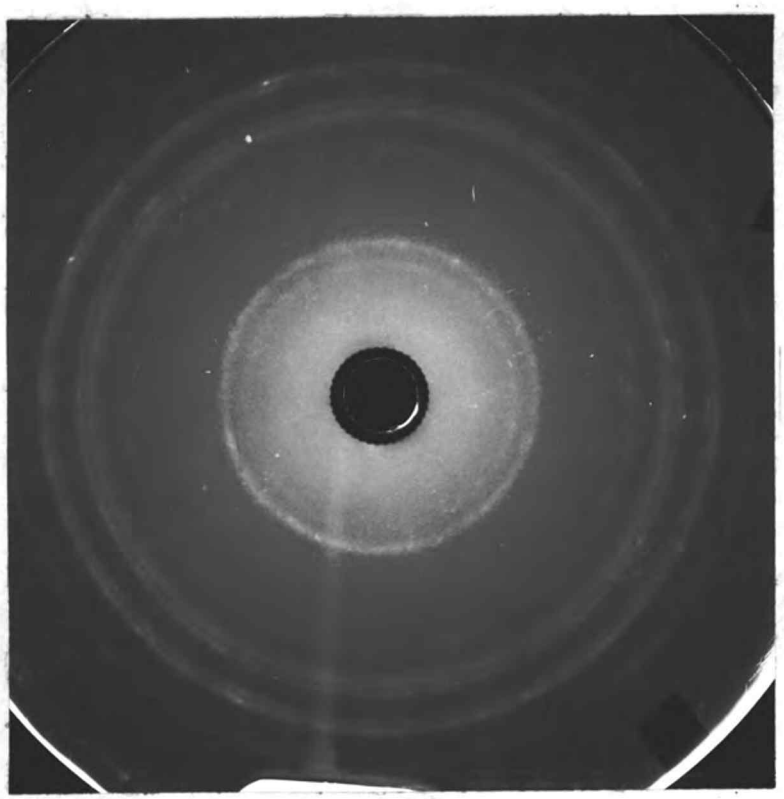

Figure 18

Specimen 4F
22,000 psi
450 F
395 hr.

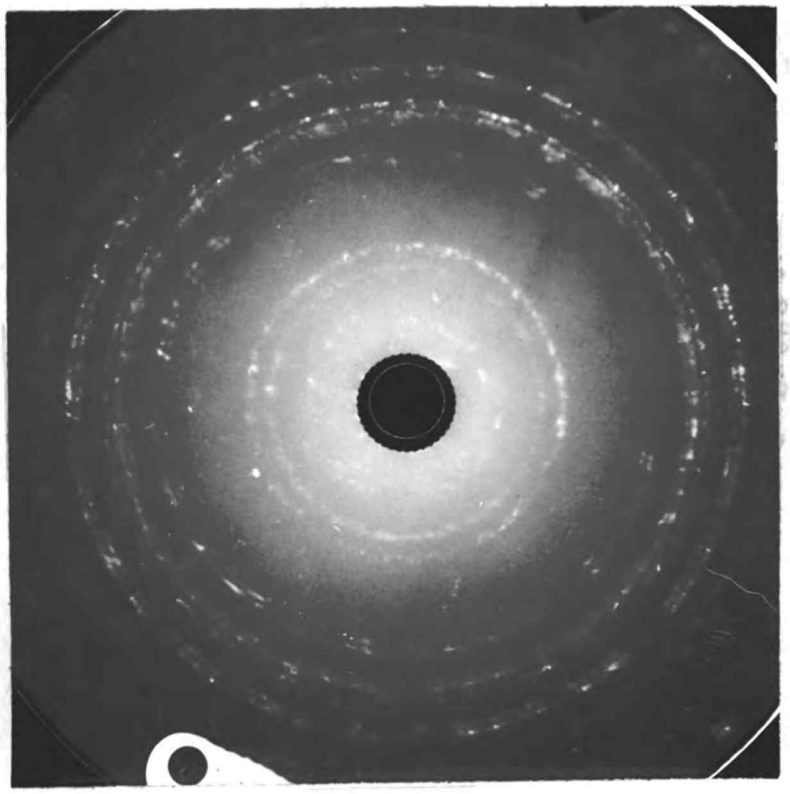

Figure 19

Specimen 4K
19,000 psi
at 485 F
500 hr.

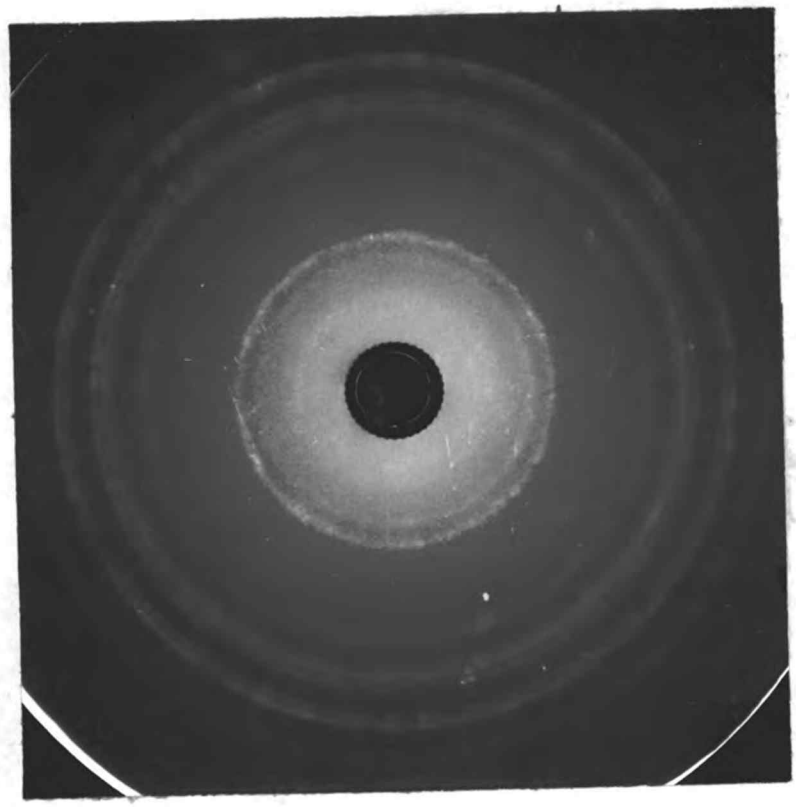

Figure 20

Specimen 4L
21,000 psi
at 475 F
500 hr.

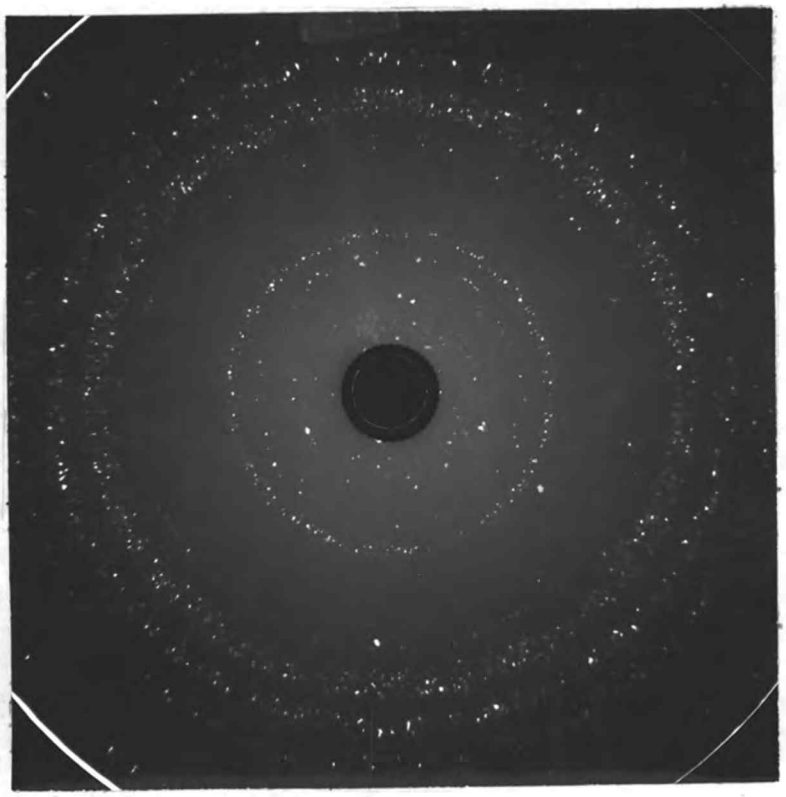

Figure 21

Specimen 40
no stress
495 F
500 hr.

Figure 22

Specimen 30
20,000 psi
at 490 F
500 hr.

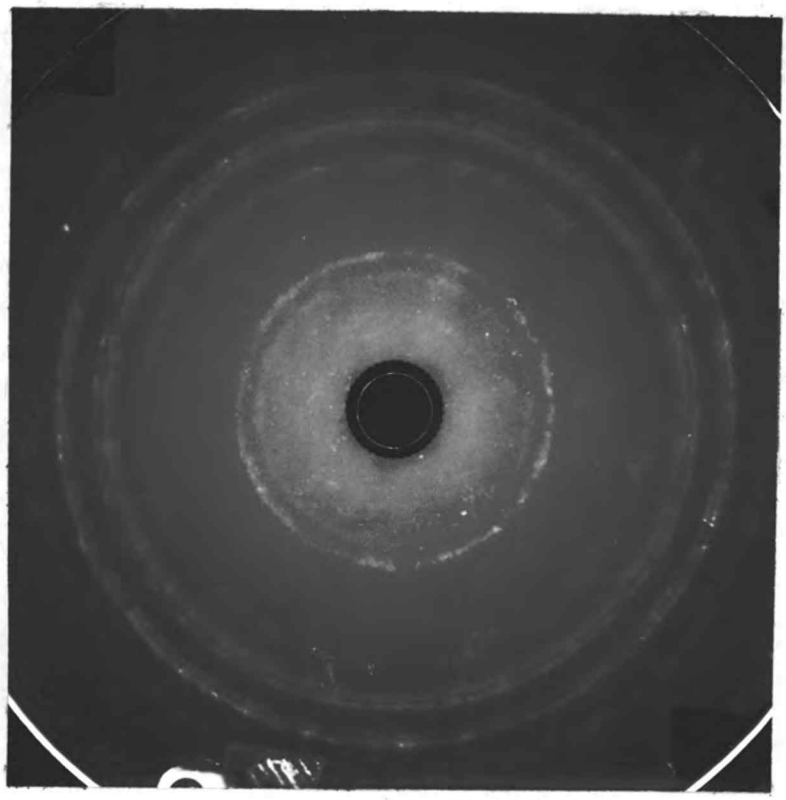

Figure 23

Specimen 3N
20,000 psi
at 490 F
500 hr.

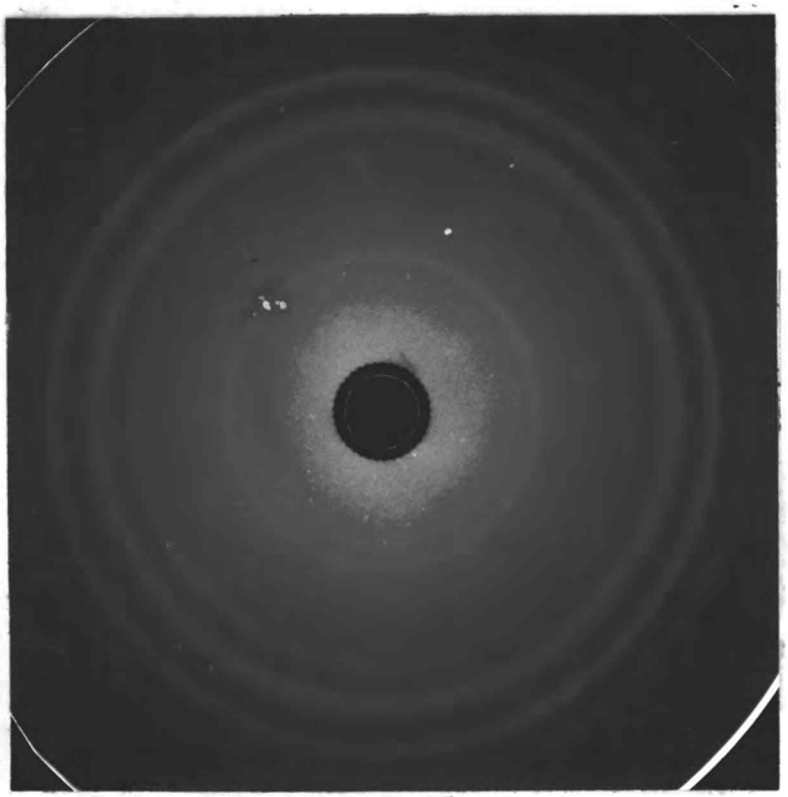

Figure 24

Specimen 3J
24,000 psi
at 485 F
broke after
26 hr.

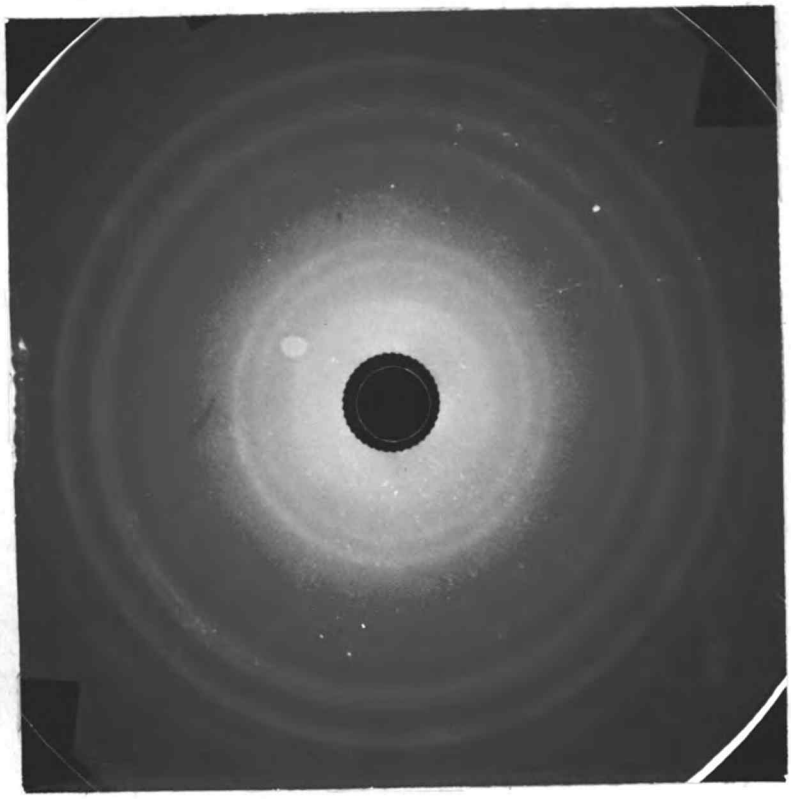

Figure 25

Specimen 3I
23,000 psi
at 486 F
broke after
120 hr.

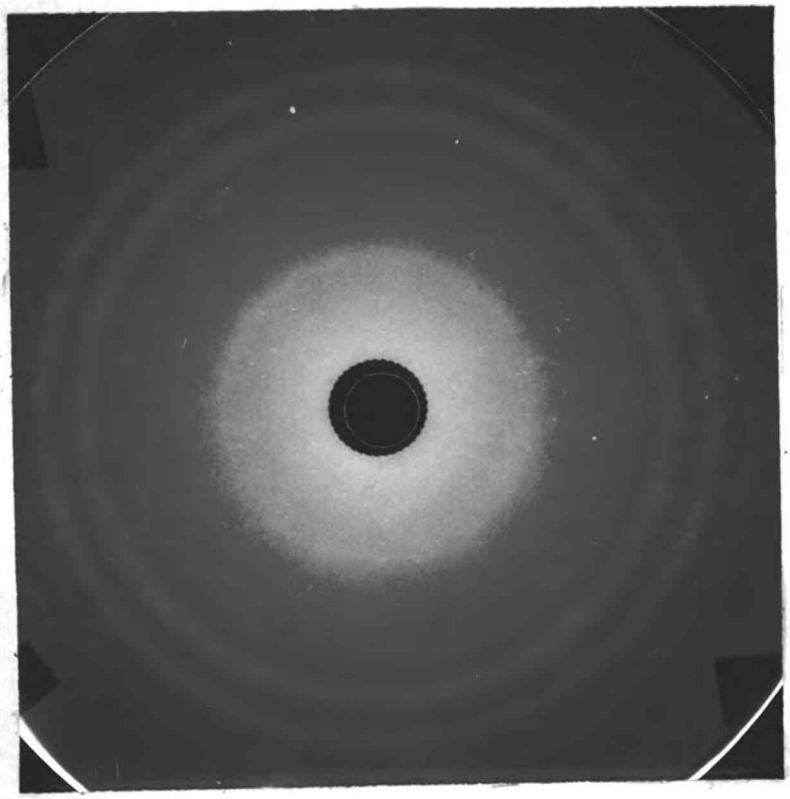

Figure 26

Specimen 4Q
no creep
after tensile
testing

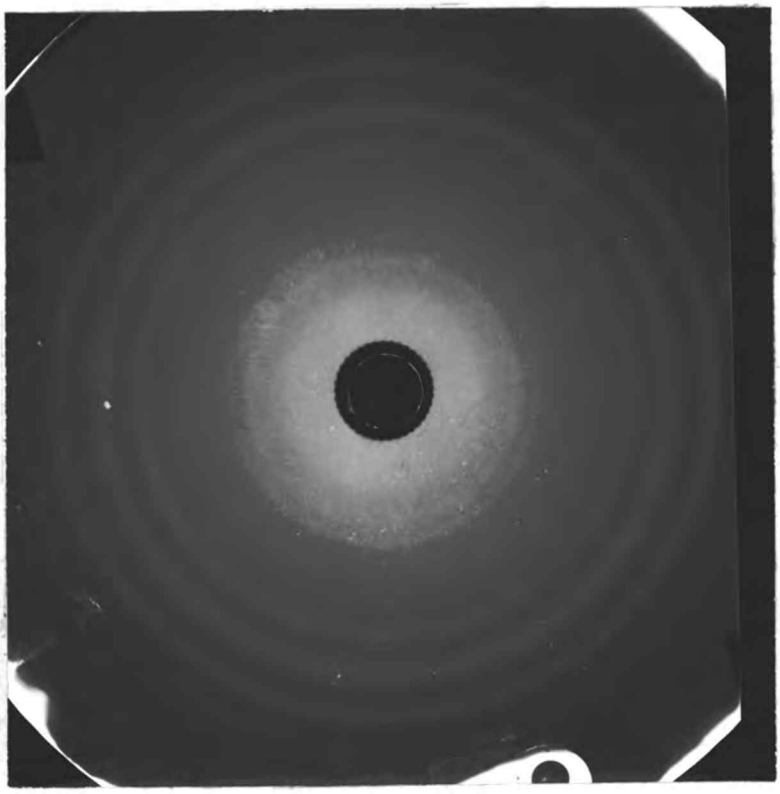

Figure 27

Specimen 3J
24,000 psi
at 485 F
broke after
26 hr.
annealed in
furnace at
485 F - 2 hr.

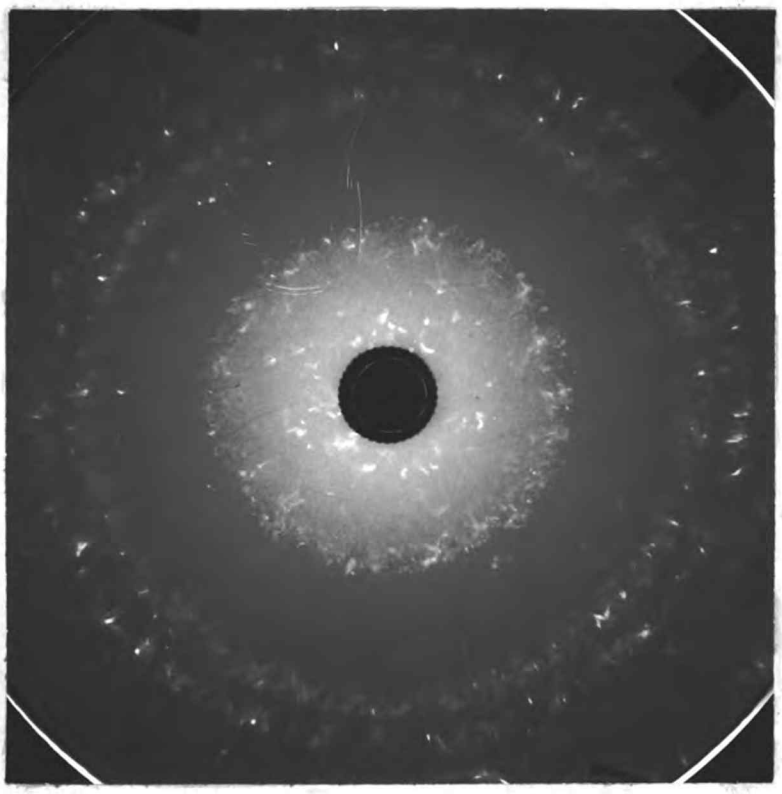

Figure 28

Specimen 3Y
no creep
tensile tested
4 per cent
elongation

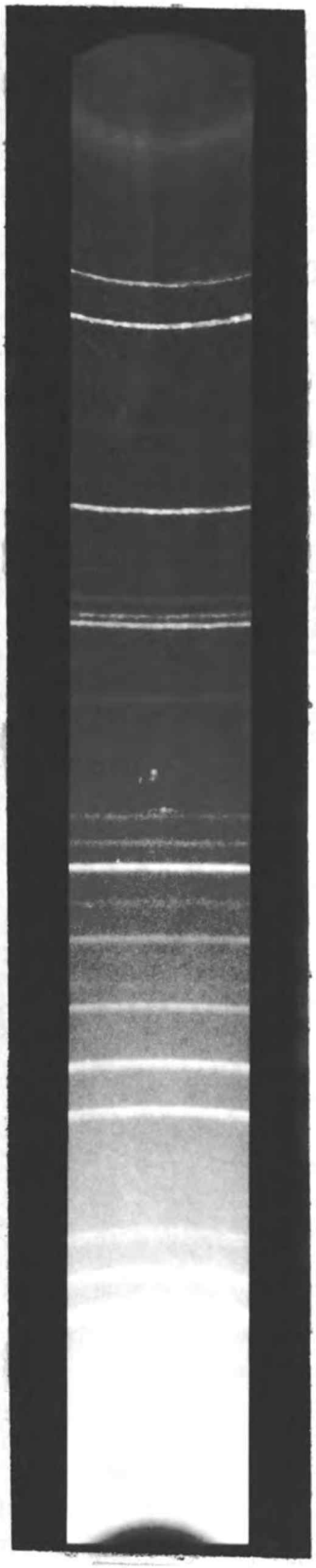

Figure 29

Powder pattern anneal specimen

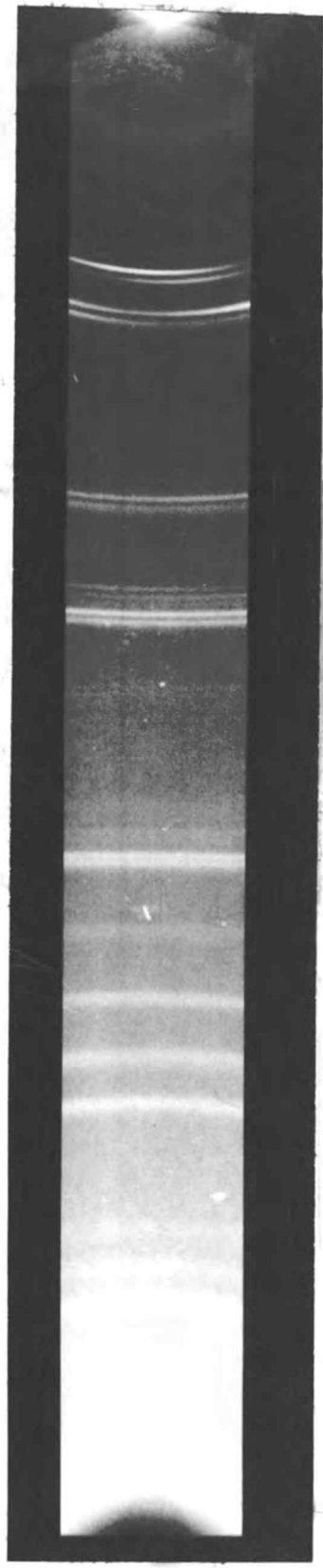

Figure 30

Powder pattern cold worked spcimen

METALLOGRAPHY

Because of the limited number of specimens, only the ruptured specimens were examined metallographically and others were used for tensile testing.

Each metallographic specimen was polished and then etched with a solution of 45 per cent nitric acid, 45 per cent water, and 10 per cent hydrofluoric acid. The clearest photographs were obtained by using polarized light, and the magnifications used were 100x and 500x. The white specks observed on all photographs are from unknown causes, probably being due to either the polishing process or impurities. Some of these specks were observed as pits under bright lighting.

Figs. 31 and 32 show the specimen in the annealed condition at 100 and 500 magnifications respectively. The grain structure in the annealed condition was the same both perpendicular and transverse to the specimen axis.

Fig. 33 is an end cross-section view of a specimen after rupturing under creep conditions. It is not representative of the entire specimen because it was taken close to the fracture. The grains seem to be greatly distorted and fragmented.

Figs. 34 and 35 are of specimen 31 which fractured after 26 hours of creep under 23,000 psi and are at 100 and 500 magnifications respectively. It is evident, when comparing Fig. 34 with Fig. 31, that the grains have been

distorted in one particular direction.

Discussion

The equipment for an exacting metallographic study was not available and consequently the subgrains mentioned previously in the x-ray section were not observable. Besides requiring special equipment, the etching process is critical and requires special techniques to reveal the subgrain formations.

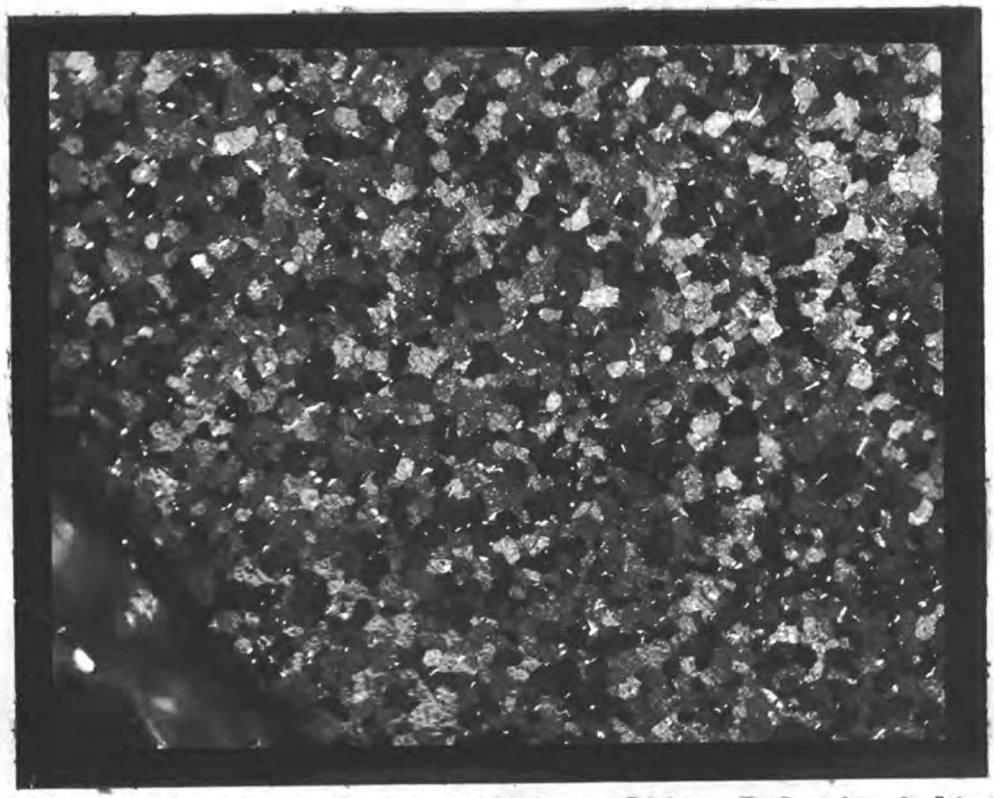

Figure 31. Annealed condition, 100x, Polarized light.

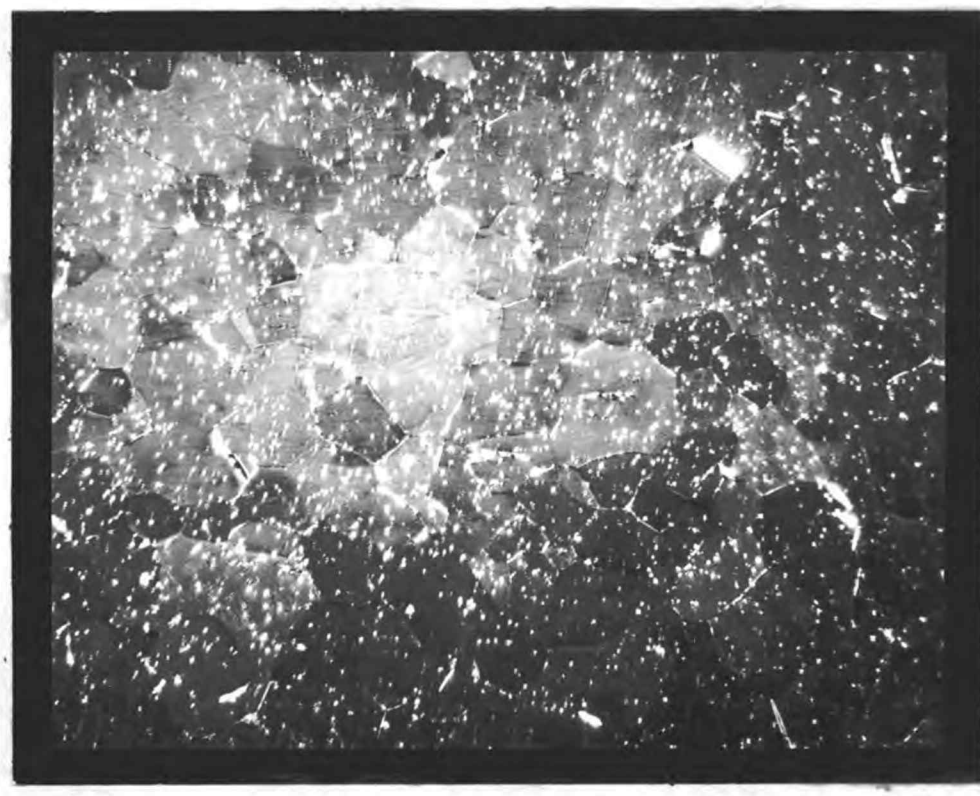

Figure 32. Annealed condition, 500x, Polarized light.

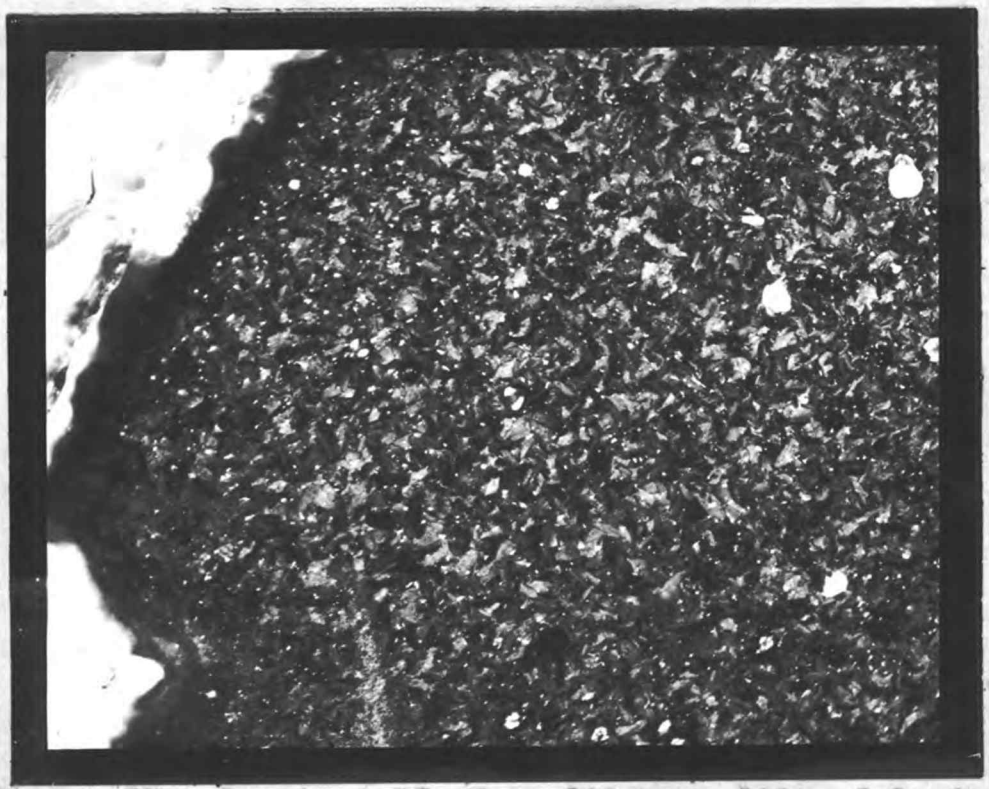

Figure 33. Specimen 3J, Fra. 100 hr., 100x, Polarized light.

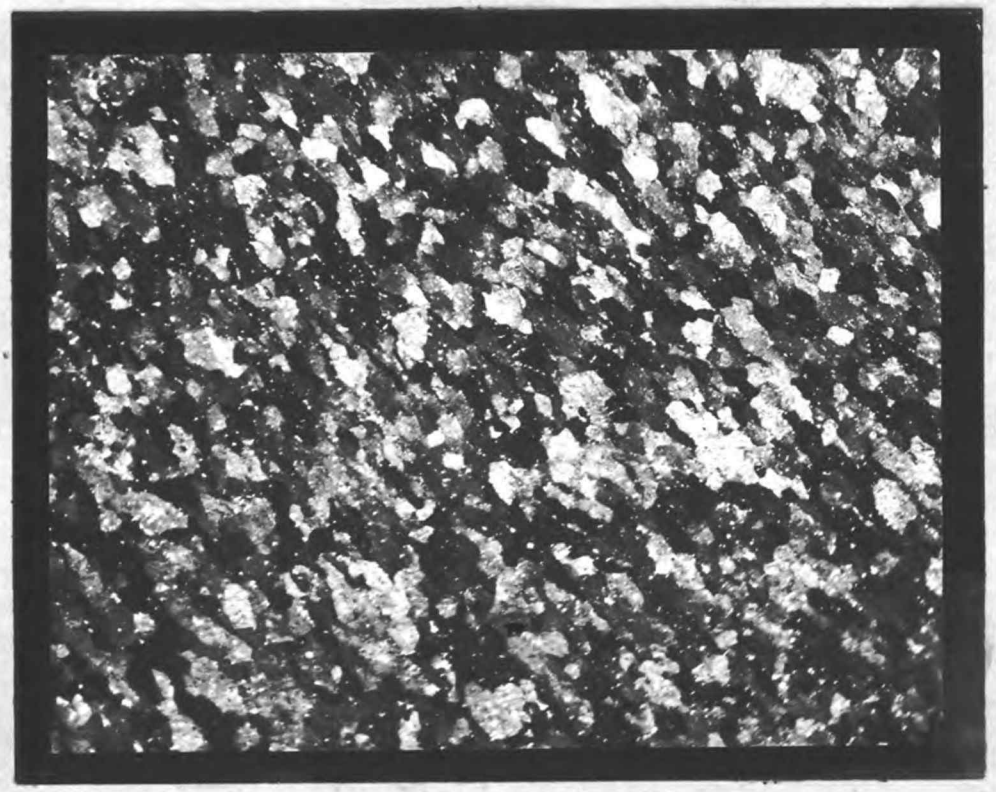

Figure 34. Specimen 3I, Fra. 26 hr., 100x, Polarized light.

Figure 35. Specimen 3I, Fra. 26 hr., 500x, Polarized light.

FINAL CONCLUSIONS

1. The creep curves determined from the experimental results were related to the logarithmic equation $\epsilon = AT^m$ where both A and n increased with increasing stress. Stress was also related to strain by the equation $\epsilon = B\sigma^m$.
2. It was determined from the creep rupture tests that the creep rupture strength of zirconium decreases with increase in initial grain size.
3. The yield strength of zirconium was increased as much as 20 per cent after being subjected to creep. The ultimate strength also increased a small amount subsequent to creep and both the ductility and modulus of elasticity were decreased after being subjected to creep conditions.
4. From the x-ray analysis a subgrain formation was detected and its formation was related to either an immediate fragmentation or a polygonization process. The experimental data were not sufficient to differentiate between the two although it may be a combination of both.
5. A line sharpening of the x-ray diffraction photographs was observed on specimens subjected to creep whereas specimens subjected to the same strain but at room temperature and at a faster rate showed very broad

diffuse lines. It was concluded that either a recovery process besides polygonization was occurring or under creep conditions the specimens did not undergo as much internal deformation which would suggest a grain boundary type of slip.

6. No noticeable changes in lattice parameters were found by use of the powder pattern.
7. The subgrain formation found by x-ray analysis was not observable metallographically and therefore more refined methods will have to be developed to reveal the substructure.
8. Both the subgrain formation, which would decrease the size of the grains, and the residual internal strain would lead to an increase in both room temperature yield and ultimate strength and would decrease the ductility.
9. No preferred orientation was observed except at the low angle diffractions.

1. Andrade, E. N. da C. The concept of creep. In: Creep and recovery. Cleveland, American Society for Metals, n.d. p. 176-198.

2. Barrett, Charles S. Structure of metals. 2d ed. New York, McGraw-Hill, 1952. 661 p.

3. Bostrom, W. A. and S. A. Kulin. Recovery of cold-worked zirconium. In: Zirconium and zirconium alloys. Cleveland, American Society for Metals, 1953. p. 186-196.

4. Cahn, R. W. Internal strains and recrystallization. In: Bruce Chalmer's (ed) Progress in metal physics. New York, Interscience, 1950. p. 151-176.

5. Chang, H. C. and N. J. Grant. Inhomogeneity in creep deformation of coarse grained high purity aluminum. Transactions of the American Institute of Mining and Metallurgical Engineers 197:1175-1180. 1953.

6. Croeni, Jack G. Creep tests on single strand aluminum alloy conductor wire. Master's thesis. Corvallis, Oregon State College, 1957. 85 numb. leaves.

7. Crussard, C. Le role des joints intergranulaires dans la deformation des metaux. Application au fluage et a la fatigue. Revue de metallurgie 43:307-316. 1946.

8. Cullity, B. D. Elements of x-ray diffraction. Reading, Addison-Wesley, n.d. 514 p.

9. Davis, Hammer E., George Earl Troxell, and Clement T. Wiskocil. Testing and inspection of engineering materials. 2d ed. New York, McGraw-Hill, 1955. 431 p.

10. Frank, F. C. On slip bands as a consequence of the dynamic behavior of dislocations. In: Report of a conference on strength of solids. London, The Physical Society, 1948. p. 46-51.

11. Gervais, Andre M., John T. Norton, and Nicholas J. Grant. Subgrain formation in high purity aluminum during creep at high temperatures. Transactions of the American Institute of Mining and Metallurgical Engineers 197: 1166-1174. 1953.

12. Gluck, Jeremy V., Howard R. Voorhees and James W. Freeman. Effect of prior creep on mechanical properties of aircraft structural metals (2024-T86 aluminum and 17-7 PH stainless). U.S. Wright Air Development Center,

WADC Technical Report 57-150, part I (Astia Document No. AD 150956) February 1958.

13. Guinier, A. Researches on the polygonization of metal. In: Bruce Chalmer's (ed) Progress in Metal Physics. New York, Interscience, 1950. p. 177-192.

14. Hanson, D. and M. A. Wheeler. The deformation of metals under prolonged loading part 1 - The flow and fracture of aluminum. The Journal of the Institute of Metals 55:229-264. 1931.

15. Hibbard, W. R. Jr. and C. G. Dunn. Polygonization. In: Creep and Recovery. Cleveland, American Society for Metals, n.d. p. 52-83.

16. Hirst, H. Deformation of single crystals of lead by creep. Part IV: Process of deformation during creep. Proceedings Australasian Institute of Mining and Metallurgy 121:11-44. Mar. 1941.

17. Homes, G. A. Recherches sur le mecanisme structurale due comportement mecanique des metaux aux temperatures elevees. Revue de Metallurgie 36:373-387. 1939.

18. Jenkins, C. H. M. and G. A. Mellor. Investigation of the behavior of metals under deformation at high temperatures. Part I: Structural changes in mild steels and commercial irons during creep. Journal of the Iron and Steel Institute 132:179-227. 1935.

19. Lustman, Benjamin and Frank Kerze. The metallurgy of zirconium. New York, McGraw-Hill, 1955. 776 p.

20. McGeary, R. K. and B. Lustman. Kinetics of thermal reorientations in cold rolled zirconium. Transactions of American Institute of Mining and Metallurgical Engineers 197:284-291. 1953.

21. Schoeck, Gunther. Theory of creep. In: Creep and Recovery. Cleveland, American Society for Metals, n.d. p. 199-226.

22. Sherby, Oleg D. and John E. Dorn. Some observations on correlations between the creep behavior and the resulting structure in alpha solid solutions. Transactions of the American Institute of Mining and Metallurgical Engineers 197:324-330. 1953.

23. Smith, Morton C. Principles of physical metallurgy. New York, Harper and Brothers, n.d. 417 p.

24. Sully, A. H. Metallic creep and creep resistant alloys. London, Butterworths Scientific, 1949. 267 p.

25. Tapsell, H. J. Creep of metals. London, Humphrey Milford, Oxford University Press, 1931. 279 p.

26. Wilder, A. B., E. F. Ketterer, and D. B. Collyer. Creep rupture properties and structural changes in carbon and low alloy steels. Transactions of the American Institute of Mining and Metallurgical Engineers 200:764-772. 1954.

27. Wood, W. A. and H. J. Tapsell. Mechanism of creep in metals. Nature 158:415-416. Sept. 21, 1946.